



Article

One-Pot Multicomponent Synthesis and Bioevaluation of Tetrahydroquinoline Derivatives as Potential Antioxidants, α -Amylase Enzyme Inhibitors, Anti-Cancerous and Anti-Inflammatory Agents

Samra Farooq , Aqsa Mazhar, Areej Ghouri, Ihsan-UI-Haq  and Naseem Ullah *

Department of Pharmacy, Faculty of Biological Science, Quaid-I-Azam University, Islamabad 45320, Pakistan; samrafarooq@bs.qau.edu.pk (S.F.); aqsamazhar1947@gmail.com (A.M.); areejkhan27@gmail.com (A.G.); ihaq@qau.edu.pk (I.-U.-H.)

* Correspondence: nullah@qau.edu.pk; Tel.: +92-334-5023566

Academic Editor: Robert Musiol

Received: 26 May 2020; Accepted: 7 June 2020; Published: 11 June 2020



Abstract: Mankind has always suffered from multiple diseases. Therefore, there has been a rigorous need in the field of medicinal chemistry for the design and discovery of new and potent molecular entities. In this work, thirteen tetrahydroquinoline derivatives were synthesized and evaluated biologically for their antioxidant, α -amylase enzyme inhibitory, anti-proliferative and anti-inflammatory activities. **SF8** showed the lowest IC_{50} of 29.19 ± 0.25 $\mu\text{g}/\text{mL}$ by scavenging DPPH free radicals. **SF5** showed significant antioxidant activity in total antioxidant capacity (TAC) and total reducing power (TRP) assays. **SF5** and **SF9** showed the maximum inhibition of α -amylase enzyme i.e., 97.47% and 89.93%, respectively, at 200 $\mu\text{g}/\text{mL}$ concentration. Five compounds were shortlisted to determine their anti-proliferative potential against Hep-2C cells. The study was conducted for 24, 48 and 72 h. **SF8** showed significant results, having an IC_{50} value of 11.9 ± 1.04 μM at 72 h when compared with standard cisplatin (IC_{50} value of 14.6 ± 1.01 μM). An in vitro nitric oxide (NO) assay was performed to select compounds for in vivo anti-inflammatory activity evaluation. **SF13** scavenged the NO level to a maximum of 85% at 50 μM concentration, followed by **SF1** and **SF2**. Based on the NO scavenging assay results, in vivo anti-inflammatory studies were also performed and the results showed significant activity compared to the standard, acetylsalicylic acid (ASA).

Keywords: tetrahydroquinoline; antioxidant; α -amylase enzyme inhibition; MTT assay; in vivo anti-inflammatory activity

1. Introduction

The field of drug discovery has conventionally been a dynamic, innovation-driven and highly prosperous sector of the global industry. Revolutionary advancements in health disciplines and technology have helped researchers in the discovery and development of numerous drugs, which play a significant role in the pharmacotherapy of a range of ailments and diseases [1]. Innovations in medicinal chemistry are responsible for the discovery of many breakthrough remedies that have ultimately improved the life and health of human beings over the past century. Continuous efforts in the development and evaluation of new molecules are required to drive the discovery of new medicines [2]. Numerous studies have been focused on the treatment of medical problems such as cancer, oxidative stress, inflammatory disorders, diabetes, etc.

The human body produces free radicals in the form of reactive oxygen species (ROS), which regulate cellular processes, i.e., angiogenesis, platelet aggregation, signal transduction, etc. When produced in excess, free radicals can impose a harmful and deleterious impact on cellular components, i.e.,

lipids, proteins, DNA, etc. This may lead to many chronic diseases, such as diabetes, cancer and atherosclerosis [3]. Antioxidants can scavenge these free radicals and helps to regulate the progression and prevention of carcinogenesis [4,5]. Cancer is an enigma that has threatened human lives for ages. It has a major impact on society across the globe as a leading cause of death worldwide. Subsequently, the amount of resources spent on its treatment is increasing daily. Therefore, enormous efforts have been invested in the research and development of anti-cancer products both in industry and academia [6].

Diabetes mellitus is one of the most common and emerging diseases in the world [7]. α -Amylase is a key enzyme responsible for the hydrolysis of carbohydrates. Inhibiting α -amylase is a successful approach to controlling postprandial blood sugar within the acceptable range, which is a key factor in controlling diabetes mellitus (DM) [8–10].

Inflammation is an indication of many pathological conditions, such as rheumatoid arthritis, osteoarthritis, Alzheimer's disease, hepatitis, cancer, pulmonary fibrosis and obesity-related diseases [11,12]. Lipopolysaccharide (LPS), a bacterial endotoxin, plays an important role during inflammation by regulating a cascade of cellular responses [13]. Throughout the inflammatory process, pro-inflammatory mediators, cytokines, nitric oxide (NO) and prostaglandin E2 are produced by the inducible isoform of nitric oxide synthase (NOS) and cyclooxygenase-2 (COX-2) [14]. NO is a free radical synthesized from L-arginine and catalyzed by iNOS [15]. Additionally, iNOS is closely associated with a variety of pathological conditions [16] and can act as a cytotoxic agent in pathological conditions [17]. Thus, the inhibition of the production of NO by iNOS can be an effective approach to treat and prevent inflammatory diseases [18].

The concept of multicomponent organic synthesis has received increased attention in organic chemistry since it provides access to diverse libraries of organic molecules [19]. Thus, multicomponent reactions have gained great importance, especially in medicinal chemistry, and are used for the preparation of novel therapeutic agents that have numerous applications [20]. Many biologically active compounds are obtained by using the multicomponent reaction (MCR) approach. The corresponding biological activities exhibited by organic molecules include antileishmanial [21], anti-inflammatory [22], ROCK inhibitors [23], neuroprotective agents [24], acetylcholinesterase inhibitors [25], antimicrobial [26–30], antioxidants [31], anti-tumor [32,33], anti-cancer [34–39] and so on.

Quinoline [40] (1-azanaphthalene) is a very significant nitrogen-containing heterocyclic ring structure in medicinal chemistry [41,42]. It has been integrated into many molecules, resulting in compounds with a broad spectrum of potential [43]. A literature survey revealed that quinoline derivatives possess a wide range of biological activities, such as anti-inflammatory, anti-malarial, anti-tumor, anti-hypertensive, anti-microbial, tyrosine PDGF-RTK inhibiting agents, anti-HIV and anti-tubercular, etc. [44–46]. Some of the promising compounds with a quinoline ring system are depicted in the Figure 1.

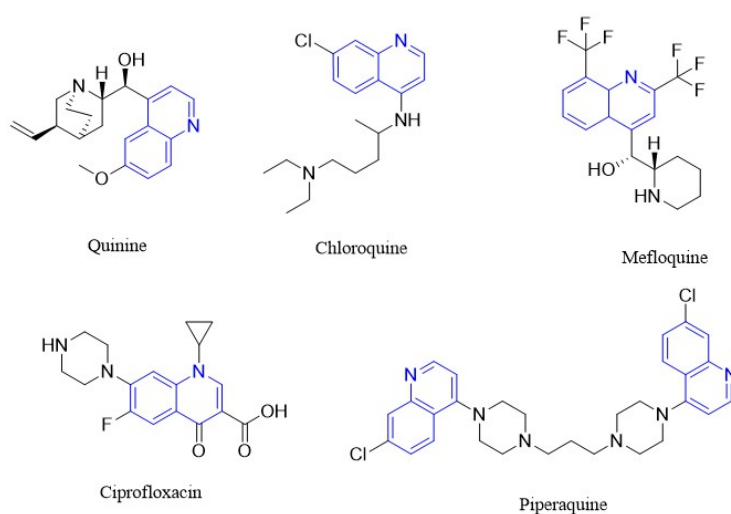


Figure 1. Selected examples of promising compounds with a quinoline ring system.

This diversity of biological effects is exhibited by benzofused six-membered heterocyclic rings. From a chemical point of view, the tetrahydroquinoline (THQ) moiety is a promising derivative of quinoline and a potential scaffold in medicinal chemistry due to its broad-spectrum biological profile, as mentioned in Figure 2. Helquinoline is a potent tetrahydroquinoline-derived antibiotic that has been extracted from *Janibacter limosus* [47]. In particular, tetrahydroquinoline exhibits a wide range of biological activities, for example, anti-HIV [48], antitrypanosomal [49], psychotropic [50], anti-inflammatory [51], antibacterial [52], antimalarial [53], antifungal [54] and antitumor activities [55].

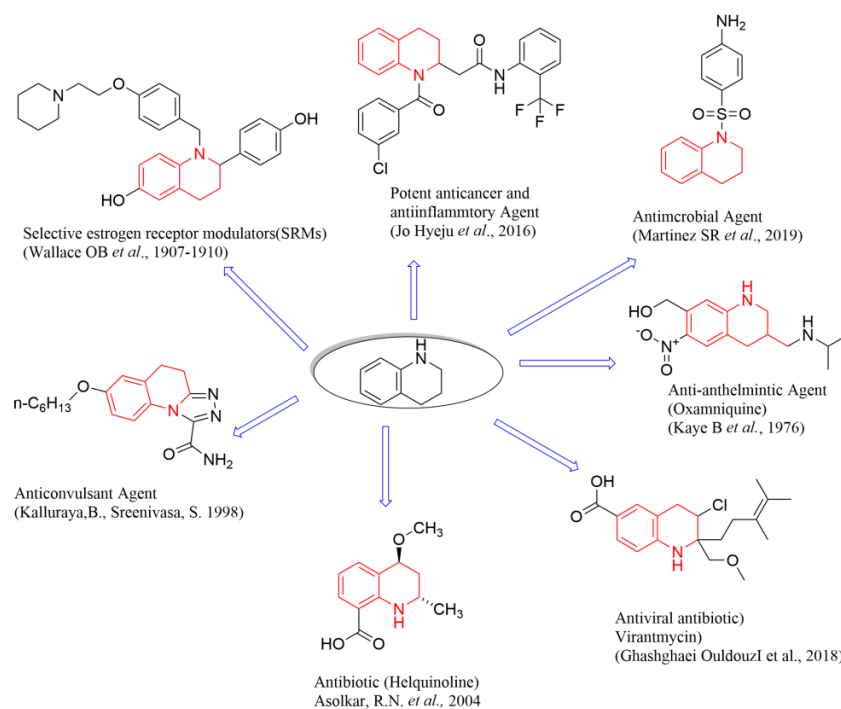


Figure 2. Selected examples of a promising tetrahydroquinoline ring system containing derivatives and their pharmacological activities.

The incorporation of a functional group into a pharmacophore is an attractive approach to the design and synthesis of new bioactive compounds. Considering the pharmacological potential of the tetrahydroquinoline moiety and our long-standing interest in exploring Mannich base chemistry [56], in the present study, we used a one-pot MCR approach to prepare a series of tetrahydroquinoline derivatives. The majority of the synthesized Mannich bases have not been reported in the literature to date. All compounds were subsequently evaluated in biological studies for their pharmacokinetic, antioxidant, α -amylase enzyme inhibition, cytotoxic and anti-inflammatory potential. The comprehensive biological profile of tetrahydroquinoline-derived N-Mannich bases by one-pot MCR reaction has not yet been thoroughly investigated. A literature survey demonstrated that there are no studies concerning the cytotoxic and anti-proliferative activities of tetrahydroquinoline-derived N-Mannich bases.

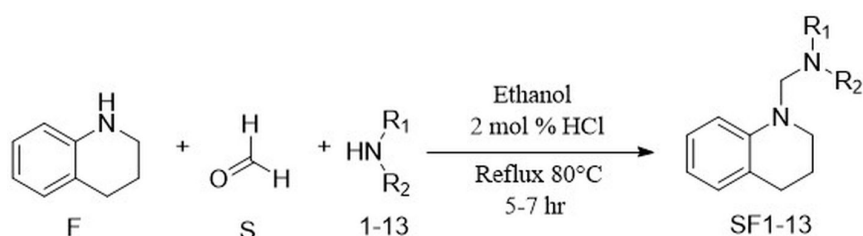
2. Results and Discussions

2.1. Chemistry

Multicomponent reactions (MCRs) are considered to be very important and powerful reactions in combinatorial and medicinal chemistry [57] because of the benefits they offer in terms of the synthesis of diverse structures that will lead to an increase in the economy of organic synthesis [58,59] by shortening the time span [60].

The reaction between aldehydes, amines or ammonia and heterocyclic acidic proton-containing pharmacophores is known as a Mannich reaction. It was reported for the first time by a German chemist, Carl Mannich, in 1912, for the synthesis of atropine glucoside [61,62].

The synthetic route used to obtain compounds (SF1–SF13) is described in Scheme 1. N-Mannich products were prepared by a one-pot, three-component condensation reaction, performed under reflux conditions. Formaldehyde (S), amine (1–13), and tetrahydroquinoline (F) were placed in a pressure tube and dissolved in ethanol and a catalytic amount of HCl was added. The mixture was refluxed at 80 °C for ~5–7 h, leading to the formation of the N-Mannich base. The product precipitated from the reaction mixture and the formed solid was separated, washed and recrystallized by ethanol. For some of the products, an additional purification step by flash column chromatography was necessary. To establish the exact position of the substituents of the titled compound, we hypothesized that the reaction was carried out at position 1, where the acidic proton-H of the parent compound reacts with the oxygen of formaldehyde (Formalin 37%) and takes one -H from the amines, yielding a water molecule as a byproduct during the reflux condensation reaction.



Scheme 1. One-pot multicomponent synthesis of 1, 2, 3, 4-tetrahydroquinoline Mannich base derivatives.

The Mannich reaction is a condensation reaction where the substrate used is XH compounds, with X being any heteroatom (C, N, S, etc.) with nucleophilic properties. The reaction is the nucleophilic addition of an amine to a carbonyl group of an aldehyde, followed by dehydration to a Schiff base, which acts as an electrophile and reacts with a compound containing an acidic proton. The reaction is an example of an S_N2 addition reaction [56]. From the structure of tetrahydroquinoline, it should be kept in mind that it contains one nucleophilic site, i.e., $-NH$. Under a basic environment, the nucleophile site gets deprotonated, which results in an increase in electronic condensation on the electronegative nitrogen atom (nucleophilic activation). Thus, the tetrahydroquinoline anion starts a nucleophilic attack on the electrophile and carries out an efficient S_N2 displacement and intramolecular cyclization. All the tetrahydroquinoline-derived Mannich bases were characterized by various spectroanalytical techniques. In the IR spectrum of quinoline derivatives, the strong bonds observed at around 1600 cm^{-1} and 1505 cm^{-1} correspond to aromatic $C=C$ stretching. The specific carbonyl peak shown by some synthetic compounds appeared at $1620\text{--}1680\text{ cm}^{-1}$. In proton NMR, aromatic protons were observed mostly downfield, near $\delta\ 6.52\text{--}7.7$ ppm, as per the substitution pattern at various positions of the aromatic ring. The methylene proton of $-N$ linkage ($N-CH_2-N$) was resonated at around $\delta\ 3.52\text{--}5.44$ ppm and gave a singlet (s). Carbon NMR further confirmed the structure of the synthesized compounds. In carbon NMR of synthetic compounds, most downfield carbon was of aromatic quinoline carbon observed near $\delta\ 115\text{--}145$ ppm. The carbon of methylene imine linkage was observed at $\delta\ \sim 69$ ppm. Solvent peaks for $CDCl_3$ and $DMSO-d_6$ were observed at $\delta\ 77.2$ ppm and 39.5 ppm, respectively. All other aromatic signals were observed at the expected regions. In the mass spectral analysis of synthetic compounds (SF1–SF13), the molecular ion peak for these compounds was observed as (M^+) for all the compounds.

2.2. ADME Predictions

Synthetic compounds were evaluated for their *in silico* ADME for the assessment of pharmacokinetic parameters. A computational tool was used for the prediction of drug-likeness and molecular properties to obtain new drug-like leads. The values are presented in Table 1.

Table 1. Lipinski's rule of five for the drug-likeness of all synthesized compounds (SF1–SF13).

Comp. No	MW ¹ (< 500)	HBA ² (< 10)	HBD ³ (< 5)	ilog (P _{o/w}) ⁴ (< 5)	Mlog(P _{o/w}) ⁵ (< 5)	Lipinski Violation
SF1	230	1	0	3.02	3.21	No
SF2	232.32	2	0	2.69	2.07	No
SF3	216.32	1	0	2.78	2.95	No
SF4	246.39	1	0	3.41	3.46	No
SF5	245.36	2	0	2.94	2.33	No
SF6	231.34	2	1	2.67	2.07	No
SF7	314.42	0	0	3.46	4.89	No
SF8	272.77	0	1	3.08	3.98	No
SF9	317.22	0	1	3.17	4.10	No
SF10	280.36	1	0	2.82	3.30	No
SF11	218.34	1	0	3.11	2.95	No
SF12	268.35	1	1	3.21	3.10	No
SF13	296.36	2	1	2.61	2.81	No

¹ MW = molecular weight, ² HBA = hydrogen bond acceptor, ³ HBD = hydrogen bond donor, ⁴ ilog (P_{o/w}): octanol–water partition coefficient, ⁵ Mlog (P_{o/w}): Moriguchi LogP (octanol–water partition).

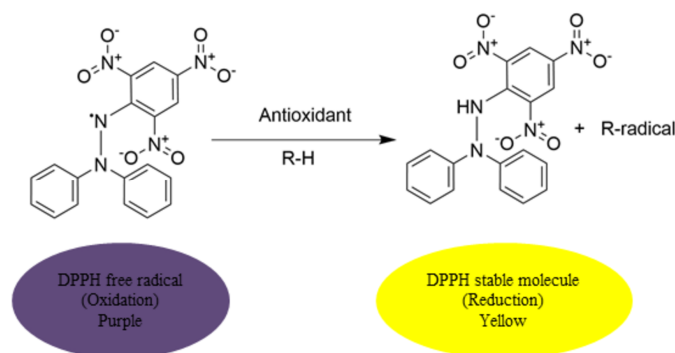
According to the biopharmaceutics drug disposition classification system (BDDCS), new molecules that are of large molecular weight, poorly water-soluble and lipophilic are categorized under BCS Class II. Lipinski et al. [63] demonstrated that molecules obtained via high-throughput screening (HTS) tend to have lipophilicity and greater molecular weights than leads in the pre-HTS era [64]. The Lipinski rule of five was developed to achieve the “drugability” of new molecular entities (NMEs) [65], which predicts that poor absorption or permeation is more likely when there are more than five H-bond donors, 10 H-bond acceptors, the molecular weight is greater than 500 and the calculated log *p* (CLog *p*) is greater than 5 [63,65]. In the current study, all the synthetic compounds were shown to have followed Lipinski's rule of five, which demonstrates that these all fulfill the basic requirement for orally active drugs and tend to have low attrition rates during clinical trials.

2.3. Bioevaluation

2.3.1. Antioxidant Assays

DPPH Assay

The % free radical scavenging activity (%FRSA) of the synthetic compounds was evaluated by the discoloration of an unstable DPPH reagent to the stable yellow-colored 2,2-diphenyl-1-picrylhydrazine molecule by accepting one electron from a donor antioxidant [66]; the mechanism is shown in Scheme 2.

**Scheme 2.** Mechanism of DPPH with an antioxidant with a transferable hydrogen radical [67].

The results of the %FRSA of the synthetic compounds and their IC₅₀ data are summarized in Table 2.

Table 2. DPPH free radical scavenging activity of synthetic compounds with IC₅₀ values.

Compound	% DPPH Scavenging Activity at Different Concentrations				IC ₅₀ (µg/mL) ^a
	200 µg/mL	66.66 µg/mL	22.22 µg/mL	7.4 µg/mL	
SF1	62.45 ± 0.12	50.08 ± 0.18	27.76 ± 0.11	11.91 ± 0.32	44.22 ± 0.25
SF2	71.85 ± 0.27	58.39 ± 0.27	36.61 ± 0.22	17.44 ± 0.26	42.55 ± 0.36
SF3	27.19 ± 0.31	18.32 ± 0.91	9.85 ± 0.18	3.76 ± 0.125	52.75 ± 0.28
SF4	58.58 ± 0.33	53.65 ± 0.14	41.63 ± 0.28	18.12 ± 0.20	29.79 ± 0.26
SF5	45.24 ± 0.28	28.77 ± 0.14	17.39 ± 0.16	7.76 ± 0.23	56.63 ± 0.32
SF6	66.61 ± 0.13	50.32 ± 0.18	37.75 ± 0.31	8.81 ± 0.21	35.89 ± 0.33
SF7	64.48 ± 0.18	50.48 ± 0.054	26.76 ± 0.17	9.28 ± 0.13	44.4 ± 0.29
SF8	62.35 ± 0.14	52.12 ± 0.36	50.17 ± 0.32	27.98 ± 0.24	29.19 ± 0.25
SF9	67.46 ± 0.14	50.28 ± 0.22	19.35 ± 0.11	7.64 ± 0.26	50.76 ± 0.37
SF10	49.73 ± 0.19	40.77 ± 0.31	31.89 ± 0.21	23.45 ± 0.28	47.81 ± 0.27
SF11	43.93 ± 0.28	30.9 ± 0.12	15.54 ± 0.09	7.76 ± 0.18	53.63 ± 0.13
SF12	64.20 ± 0.31	54.10 ± 0.17	31.80 ± 0.42	11.24 ± 0.11	39.33 ± 0.28
SF13	19.34 ± 0.34	11.78 ± 0.15 s	4.44 ± 0.18	1.98 ± 0.20	60.78 ± 0.36
Blank	0	0	0	0	–
Ascorbic Acid	89.01 ± 0.18	76.63 ± 0.19	52.12 ± 0.31	31.35 ± 0.23	41.38 ± 0.34
Quercetin	81.43 ± 0.21	69.81 ± 0.17	58.31 ± 0.28	42.34 ± 0.36	41.64 ± 1.01

^a required concentration of the tested compounds to scavenge 50% of the DPPH radicals; values are mean ± SEM (standard error of the mean, *n* = 3).

All the synthetic compounds were shown to scavenge the DPPH free radical to some extent. **SF8**, which has an electronegative atom, was shown to have the most potent effect, with an IC₅₀ value of 29.19 ± 0.25 µg/mL, which was lower than the standard, ascorbic acid and quercetin, with values of 41.38 ± 0.34 and 41.64 ± 1.01 µg/mL, respectively. Among the other synthetic series, **SF4**, **SF6** and **SF12** exhibited good antioxidant potential against DPPH free radicals, with IC₅₀ values of 29.79 ± 0.26, 35.89 ± 0.33 and 39.33 ± 0.28 µg/mL, respectively. These characteristic results could be because of the formation of the hydrogen bond between an amine and a lone pair of nitrogen present on an unstable DPPH free radical. The high activity of aromatic amines is because of their ability to form nitroxyl radicals [68]. The literature survey supports the results of **SF6** and **SF8** being good antioxidants because of the nature of their substituents, i.e., electron-withdrawing (chlorine in **SF8**) and electron-donating (piperazine moiety in **SF6**) groups attached to the heterocyclic core [69].

Phosphomolybdenum-Based Total Antioxidant Capacity (TAC) and Total Reducing Power (TRP)

In the presence of an antioxidant, the phosphomolybdate ion gets reduced and a green phosphate–molybdate complex is formed, which is analyzed spectrophotometrically [70]. The highest TAC was found to be 285.46 ± 2.1 µg/AAE for **SF5** bearing a methyl piperazine moiety, followed by **SF7–SF9** and **SF12**, with TAC values of 242.77 ± 2.31 µg/AAE, 212.71 ± 231 µg/AAE, 179.76 ± 1.6231 µg/AAE and 191.19 ± 1.1231 µg/AAE, respectively (Figures 3 and 4 (standard curve)).

A TRP assay was carried out to evaluate the reducing potential of synthetic compounds. The method implicates reductones. These reductones are species with antioxidant potential that is believed to be due to their proton-donating capacity [71]. This results in a discontinuation of a free radical chain. The maximum value of reducing power was 104.7 ± 1.9 µg/AAE for **SF5**, followed by 103.18 ± 2.4 µg/AAE for **SF7** and 84.57 ± 1.9 µg/AAE for **SF12** (Figures 3 and 4 (standard curve)). The results indicate that synthetic compounds have the potential to stabilize free radicals by donating electrons and exhibited reductive potential with the highest reducing power [72]. The lowest reducing potential was observed for **SF1**, i.e., 33.22 ± 1.5 µg/AAE. **SF10** showed no activity in this assay. **SF7**, with a diphenylamine moiety, showed the highest activity in antioxidant assays due to the reason that secondary amines with an aromatic ring and nitrogen atom attached to them are good antioxidants [73] and are considered as singlet oxygen scavengers [74].

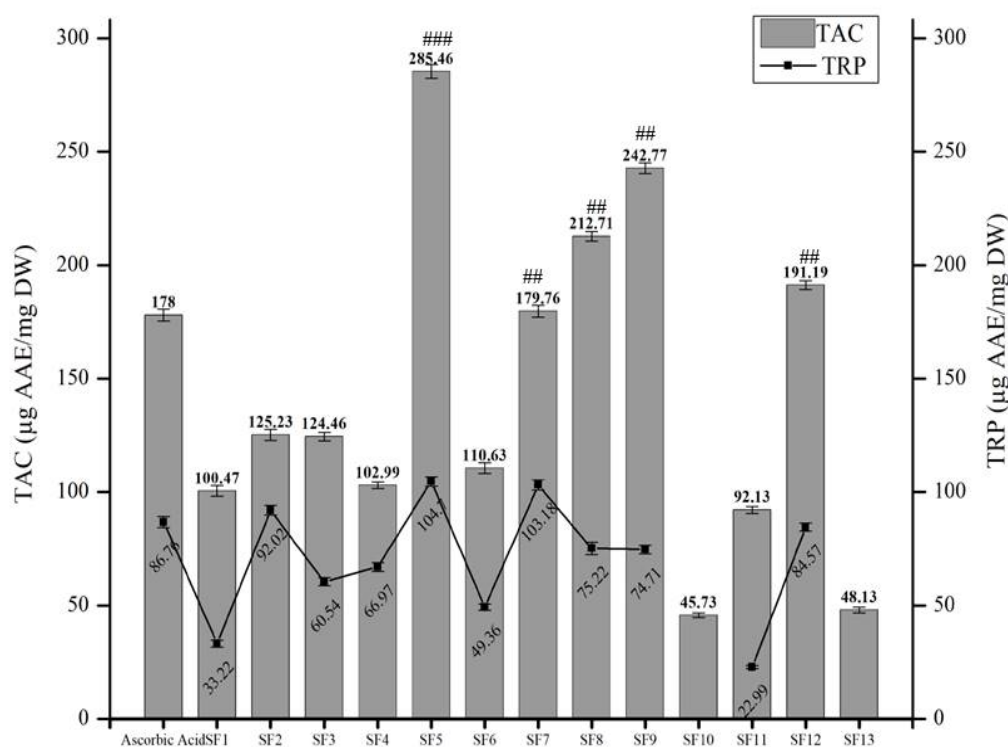


Figure 3. Ascorbic acid equivalent (AAE) antioxidant values, expressed as µg/mL. The symbol ### indicates the significance of results where $p < 0.01$, ## $p < 0.05$.

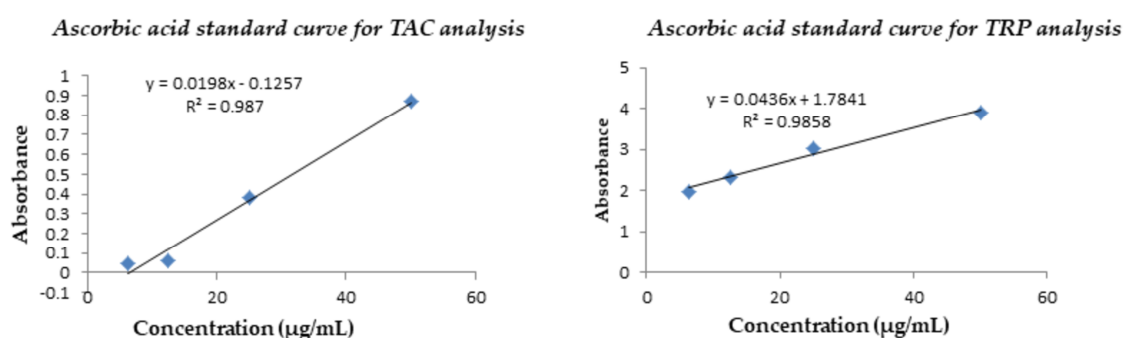


Figure 4. Ascorbic acid calibration curves ($y = 0.0198x - 0.1257$, $R^2 = 0.987$) for total antioxidant capacity (TAC) and ($y = 0.0436x + 1.7841$, $R^2 = 0.9858$) for total reducing power (TRP) estimations.

2.3.2. α -Amylase Inhibitory Assay

In the present research, the inhibition of the α -amylase enzyme was assessed *in vitro*. The results are depicted in Figure 5.

Among the tested compounds, SF5 showed the maximum % enzyme inhibition of 97.37%, followed by SF9 and SF7, with 93%, and 88.67%, respectively. SF2 showed a % enzyme inhibition close to the standard, acarbose, i.e., 79.97%. However, SF13, with an acetaminophen moiety, showed the lowest enzyme inhibition, i.e., 10.51%. The IC_{50} data were calculated by GraphPad Prism software. SF5 showed the most potent value compared to the standard, acarbose (38.05 ± 0.98 µg/mL), followed by SF9 and SF8, i.e., 18.55 ± 0.89 and 27.39 ± 1.43 µg/mL, respectively.

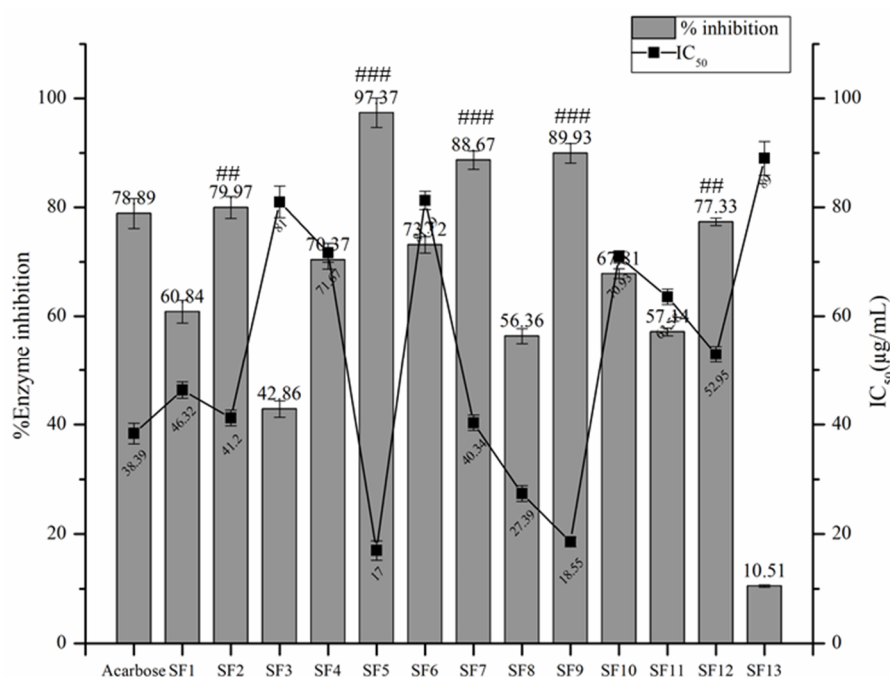


Figure 5. % inhibition of α -amylase enzyme by a library of synthetic compounds and a reference amylase inhibitor, acarbose (values are expressed as \pm SEM, $n = 3$), ### indicates the significance of results where $p < 0.01$, ## $p < 0.05$.

2.3.3. Evaluation of Cytotoxic Potential

Brine Shrimp Cytotoxicity Assay

Cytotoxicity via a brine shrimp lethality assay was studied to reveal the cytotoxicity potential of the synthetic compounds. Toxicity to brine shrimps has a direct correlation with anti-cancer activity [75]. The brine shrimp larvae correspond to the mammalian system [76] since the DNA-dependent RNA polymerases of *Artemia salina* have been reported to be similar to the mammalian type [77]. This test is not only used to predict the anti-cancer potential of corresponding compounds but also anti-microbial and pesticidal behavior [78].

Thirteen of the newly synthesized compounds were screened against brine shrimp nauplii. The cytotoxicity of synthetic compounds was determined by calculating the median lethal concentration, LD₅₀ (concentration at which 50% of the nauplii died). The results are shown in Table 3, indicating that SF5, SF4, SF7 and SF3 have good activity against brine shrimp nauplii, in comparison to a standard, doxorubicin (124 ± 1.54 $\mu\text{g/mL}$), with LD₅₀ values of 94 ± 1.06 , 100 ± 1.78 , 100.8 ± 1.14 and 102 ± 1.98 $\mu\text{g/mL}$, respectively, which corresponds to a high toxicity against cancer cells. SF1 and SF8 showed moderate toxicity, 120.8 ± 2.3 $\mu\text{g/mL}$ and 123.4 ± 1.87 $\mu\text{g/mL}$, respectively. The rest of the compounds exhibited weaker activity and were considered to be safe or non-toxic. Further cytotoxicity of the compounds was evaluated using cancer cell lines (Hep-2C).

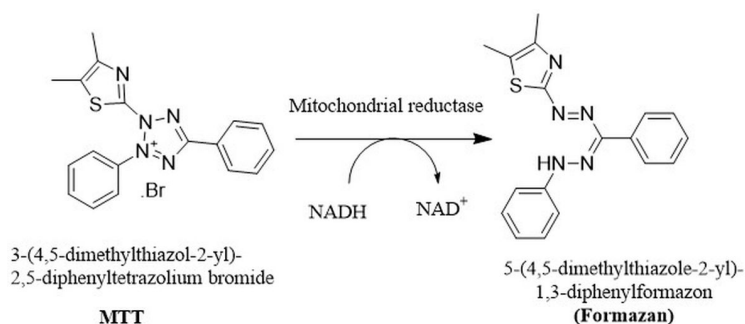
Table 3. Cytotoxicity of compounds (SF1–SF13) using brine shrimp lethality bioassay.

Compounds	LD ₅₀ (µg/mL) ± SEM ¹
SF1	120.8 ± 2.3
SF2	141.4 ± 2.1
SF3	102 ± 1.98
SF4	100 ± 1.78
SF5	94 ± 1.06
SF6	121.2 ± 1.09
SF7	100.8 ± 1.14
SF8	123.4 ± 1.87
SF9	139 ± 0.87
SF10	196.1 ± 1.12
SF11	200 ± 2.11
SF12	128 ± 1.87
SF13	204 ± 1.67
Doxorubicin	124 ± 1.54

¹ SEM = standard error of the mean, *n* = 3.

Cytotoxicity Against Raw Macrophages and Cancer Cell Lines (Hep-2C)

Before the screening studies for the % cell viability inhibition against Hep-2C, it was essential to perform cytotoxicity tests against raw macrophages to determine the toxic and non-toxic behavior of every compound. The compounds that showed the lowest IC₅₀ are considered to be toxic, as compared to the reference drug, and are screened out against cancer cells. The mechanism is depicted in Scheme 3.



Scheme 3. Conversion of MTT into formazan crystals by mitochondrial reductase enzyme.

The % cell viability of the synthetic library was evaluated *in vitro* by measuring the mitochondrial dehydrogenase activity (MTT test) on raw macrophages. All the compounds were shown to have a dose-dependent dose response (Table 4).

A 100 µM concentration was considered to be toxic for compounds because of the least number of viable cells. To determine the concentration required to achieve a 50% inhibition of cells induced by each compound, IC₅₀ values (µM) were determined and their results were compared with a cytotoxic drug, i.e., doxorubicin. SF1, SF4, SF5 and SF9 exhibited the most potent activity, with IC₅₀ values of 6.232 ± 0.01, 7.208 ± 0.05, 6.181 ± 0.05 and 14.24 ± 0.26 µM, respectively, while the standard drug doxorubicin had an IC₅₀ value of 17.08 ± 0.37 µM, conclusively, which was considered toxic for cells. The activity of the most potent compounds, SF1 and SF5, was three times more than that of doxorubicin. Piperidine-bearing compounds are known to have significant anti-cancer potential, as proved in the literature [79]. From the previous data, it is evident that the electronegativity of the substituents at the heterocyclic ring steer the magnitude of activity [80], as in the case of SF9 with an electronegative bromine atom in it. The method is not specific to anti-tumor activity. However, a positive correlation was found between the least cell viability and the cytotoxicity toward some cancer cell lines [81].

Table 4. Cell cytotoxicity of synthetic compounds at different concentrations.

Compound	% Cell Viability at Different Concentrations				IC ₅₀ (μM) ^a
	100 μM	50 μM	10 μM	1 μM	
SF1	44.66 ± 0.5	47 ± 0.84	48 ± 1.34	58 ± 0.76	6.23 ± 0.01 ***
SF2	50 ± 1.52	60 ± 0.91	70 ± 0.91	76 ± 0.46	26.80 ± 0.30
SF3	41 ± 1.07	72 ± 1.34	78 ± 0.74	83 ± 0.63	29.13 ± 0.50
SF4	39 ± 0.88	42 ± 0.87	53 ± 0.63	79 ± 0.92	7.20 ± 0.05 ***
SF5	60 ± 1.20	67 ± 0.84	74 ± 0.42	98 ± 1.01	6.18 ± 0.05 ***
SF6	60 ± 1.21	65 ± 0.76	87 ± 0.82	91 ± 0.99	23.37 ± 0.17
SF7	58 ± 0.83	84 ± 0.77	95 ± 0.96	96 ± 0.89	18.64 ± 0.13 **
SF8	52 ± 1.00	68 ± 0.79	83 ± 0.78	97 ± 1.04	21.23 ± 0.33 **
SF9	82 ± 0.96	84 ± 1.21	91 ± 0.91	98 ± 0.87	14.24 ± 0.26 **
SF10	76 ± 1.20	80 ± 1.24	95 ± 0.93	100 ± 0.88	24.82 ± 0.269
SF11	41 ± 0.83	62 ± 1.20	82 ± 0.84	95 ± 0.91	26.36 ± 0.31
SF12	41 ± 0.86	57 ± 0.89	84 ± 0.87	87 ± 0.82	35.10 ± 0.50
SF13	60 ± 1.24	73 ± 1.01	82 ± 0.66	85 ± 0.93	41.43 ± 0.69
Control	100	100	100	100	0
Doxorubicin	17 ± 0.83	33 ± 1.01	40 ± 0.87	51 ± 1.34	17.08 ± 0.37 ***

^a Values are mean ± SEM (standard error of the mean, *n* = 3, *** indicates significance at *p* < 0.01 and ** indicates significance at *p* < 0.05.

MTT Assay Against Hep-2C Cells

From the results of the brine shrimp assay and cell cytotoxicity, compounds that showed significant activity and the lowest IC₅₀ values in both assays were shortlisted for further analysis against Hep-2C cells. SF1, SF4, SF5, SF7 and SF8 showed cytotoxicity against brine shrimp nauplii at IC₅₀ values of 120 ± 2.3, 100 ± 1.78, 94 ± 1.06, 100.8 ± 1.14 and 123.4 ± 1.87 μg/mL, respectively. The same five compounds showed good cytotoxic profiles against raw macrophages at IC₅₀ values of 6.232 ± 0.01, 7.208 ± 0.05, 6.181 ± 0.05, 18.6 ± 0.13 and 21.23 ± 0.33 μM, respectively.

The results were plotted against % cell viability of Hep-2C cells and sample concentration, while cisplatin was taken as a standard (Figure 6). From the achieved results, it was clear that SF1, SF4 and SF7 exhibited better activity against the cell lines than SF5 and SF8. All other compounds were not considered to have anti-cancer potential. The anti-cancer activity was determined at 24, 48 and 72 h (Figure 6). The anti-proliferative activity of Mannich bases is supposed to be due to the formation of enones [82].

IC₅₀ values were determined by GraphPad software and plotted against time intervals (24 h, 48 h and 72 h) as summarized in Table 5. Previous data proved that heterocyclic compounds bearing piperidine in their structure are highly cytotoxic (SF1) [83]. Electronegative atoms impart moderate anti-tumor activity to compounds [16], as in SF8, which has a -chloro group in it. Electronegative or electron-withdrawing atoms will lead to an increase in cytotoxic potential (bromine, chlorine, fluorine, etc.). The structure–activity relationship (SAR) was established from these findings, which states that by derivatizing the already reported anti-cancerous lead molecule with secondary amines of cytotoxic potential will impart more cytotoxicity activity to the new product that has both nuclei. The observation of microscopic analysis of MTT stained cells and crystals is depicted in Figure 7.

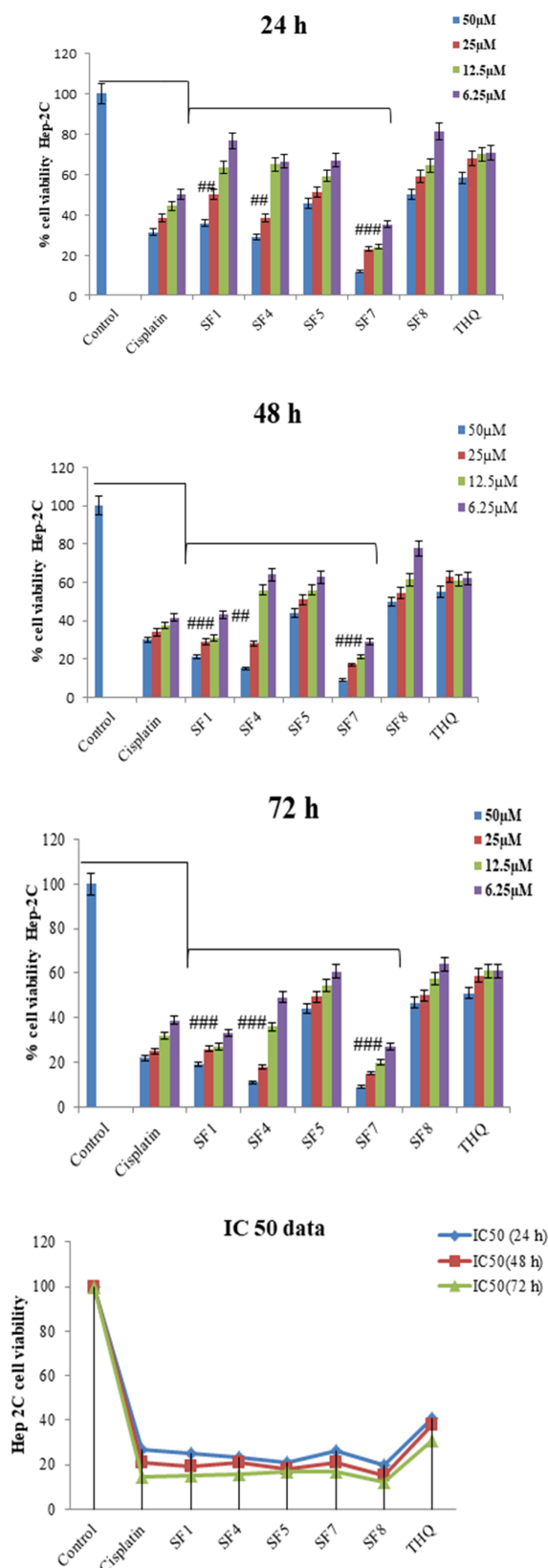


Figure 6. A 3-(4, 5-dimethylthiazol-2-yl)-2, 5-diphenyltetrazolium bromide (MTT) spectrophotometric assay of compounds (SF1, SF4, SF5, SF7, SF8) at 50, 25, 12.5 and 6.25 μM concentration in Hep-2C cells. Data are reported as mean ± SD of each compound tested in triplicate. The symbols ####/### indicates significance at $p < 0.01$ and $p < 0.05$, respectively.

Table 5. IC₅₀ data of synthetic compounds at 24, 48 and 72 h.

Compound	IC ₅₀ (μM) ¹ (Mean ± SEM) Hep-2C Cells		
	24 h	48 h	72 h
SF1	27.98 ± 1.07	21.82 ± 1.1	14.82 ± 1.07 **
SF4	23.94 ± 1.07	21.15 ± 1.2	15.53 ± 1.03 **
SF5	21.3 ± 1.09	18.02 ± 1.05	16.78 ± 1.07
SF7	26.68 ± 1.10	21.57 ± 1.05	16.81 ± 1.03
SF8	20.23 ± 1.07	15.73 ± 1.08	11.90 ± 1.04 **
THQ	41.27 ± 1.4	38.54 ± 1.23	31.98 ± 1.12
Cisplatin	19.12 ± 1.06	17.47 ± 1.07	14.63 ± 1.01 **

¹ Values are calculated as standard error of the mean (SEM), ** indicates significance at $p < 0.05$.

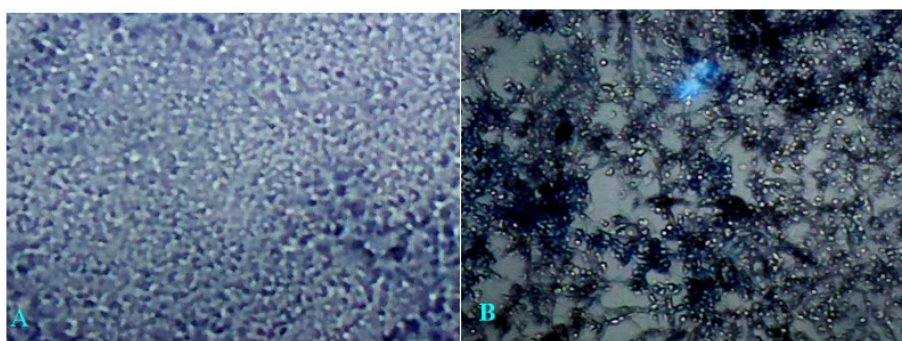


Figure 7. Characteristic images of Hep-2C cells before (A) and after (B) MTT treatment. Cells with MTT solution showed dark purple crystal formations inside of the cells.

2.3.4. Anti-Inflammatory Activity

Nitric Oxide Scavenging Assay (NO)

Nitric oxide (NO) is an indicator of inflammation. It is an important chemical mediator produced by endothelial cells, macrophages and neurons, and is involved in the regulation of many different physiological processes [84]. An excess amount of nitric oxide (NO) is associated with several diseases, i.e., inflammation, cancer and other pathological conditions. Therefore, NO production inhibition is a principle key factor for the screening of drugs with anti-inflammatory potential [85].

A Griess reagent, a spectrophotometric determination of nitrite level, was carried out to measure the nitrite level in the conditioned medium of macrophages treated with lipopolysaccharide (LPS). Sodium nitrite (NaNO₂) was used as a standard compound for the standard curve (Figure 8). The NO concentrations were obtained using the standard curve equation: $y = 0.0083x + 0.0017$, $R^2 = 0.9999$, where y is the absorbance at 540 nm and x is the NO concentration in μM. The inhibitory activity of the tested compounds towards NO generated by LPS-induced macrophages was obtained from the calculated value of x .

The highest concentration to determine the inhibition of NO production was considered to be 100 μM, and from the results summarized in Table 6, it is evident that the synthetic compounds showed the concentration-dependent response. Among the thirteen compounds, the ones that inhibited the NO production to a greater extent even at 1 μM were considered to be potent and were considered for further in vivo assays.

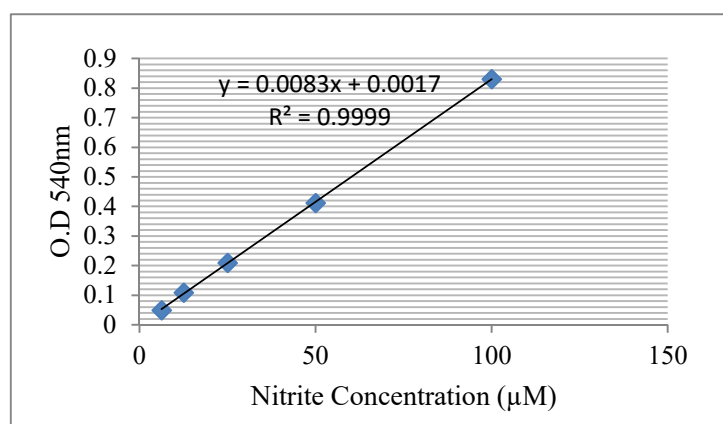


Figure 8. NaNO_2 standard curve used to obtain NO concentration.

Table 6. Nitric oxide scavenging activity of synthesized compounds at different concentrations.

Compound	Concentration (μM) and % NO Production (Mean \pm SEM) ¹			
	100	50	10	1
Piroxicam	13.351 \pm 0.54	16.457 \pm 0.41	20.710 \pm 0.24	25.35 \pm 0.45
SF1	17.313 \pm 0.35	23.687 \pm 0.41	26.0406 \pm 0.43	27.77 \pm 0.46 ***
SF2	15.345 \pm 0.29	22.091 \pm 0.33	27.093 \pm 0.36	32.23 \pm 0.34 ***
SF3	19.67 \pm 0.37	23.810 \pm 0.39	29.571 \pm 0.42	33.17 \pm 0.47 **
SF4	20.226 \pm 0.28	32.045 \pm 0.31	39.172 \pm 0.38	43.03 \pm 0.41
SF5	21.924 \pm 0.38	28.644 \pm 0.44	43.036 \pm 0.45	51.43 \pm 0.48
SF6	52.437 \pm 0.49	61.110 \pm 0.54	72.333 \pm 0.59	77.30 \pm 0.62
SF7	17.455 \pm 0.45	21.382 \pm 0.48	63.122 \pm 0.61	69.71 \pm 0.65
SF8	15.031 \pm 0.33	24.111 \pm 0.41	29.351 \pm 0.44	39.40 \pm 0.48
SF9	49.073 \pm 0.45	55.601 \pm 0.51	58.541 \pm 0.55	66.97 \pm 0.61
SF10	33.842 \pm 0.33	42.487 \pm 0.54	58.512 \pm 0.59	62.40 \pm 0.65
SF11	25.701 \pm 0.44	33.701 \pm 0.53	39.799 \pm 0.61	42.97 \pm 0.66
SF12	23.203 \pm 0.55	26.522 \pm 0.578	32.310 \pm 0.59	49.70 \pm 0.61
SF13	14.494 \pm 0.44	15.572 \pm 0.47	22.153 \pm 0.52	25.10 \pm 0.59 ***

¹ Data are presented as standard error of the mean (SEM), $n = 3$, ***/** indicate significance at $p < 0.01$ and $p < 0.05$, respectively.

The results from this finding showed that SF13 has the highest NO inhibitory potential, with the maximum inhibition of 75% at 1 μM , followed by SF1 and SF2, with NO production at 1 μM concentration of 27.771 ± 0.45 and 32.231 ± 0.46 , respectively (Table 6).

The higher NO inhibition by the synthetic compounds corresponds to the epidemiological data that suggest that lower incidences of certain inflammatory diseases, i.e., cancer, arthritis, diabetes and acquired immune deficiency syndrome (AIDS) [86,87]. These results indicate that SF13 and SF1–SF3, with acetaminophen, piperidine, morpholine and pyrrolidine amine incorporated into the basic tetrahydroquinoline ring, may suppress NO generation to a maximum extent by inhibiting iNOS enzyme activity. It is considered that the tested compounds that have shown the maximum decrease in NO production have beneficial therapeutic effects in the management of inflammatory conditions. Based on the results of NO, compounds were selected for in vivo anti-inflammatory activity.

In Vivo Anti-Inflammatory Activity

Synthetic compounds that have significantly inhibited the % nitric oxide (NO) production were further assessed for in vivo anti-inflammatory activity. Dose optimization results showed that doses of 0.1 and 1 mg/kg did not show any significant decrease in inflammatory behavior. However, at 10 mg/kg

there was a significant decrease in paw edema (Figure 9). That is why the 10 mg/kg dose was selected for further study.

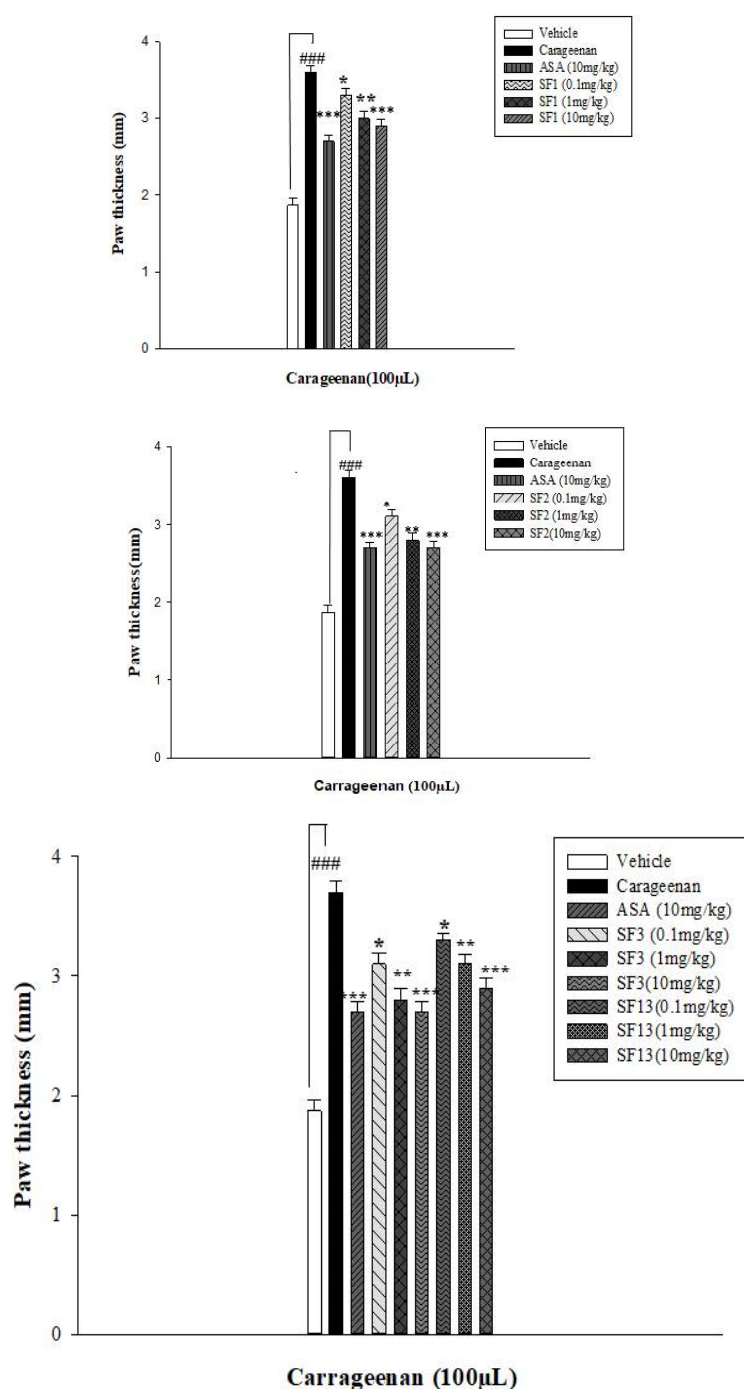


Figure 9. The dose response of synthesized compounds at 0.1, 1 and 10 mg/kg i.p. carrageenan-induced (100 µL/paw) acute inflammatory model in mice ($n = 5$). To determine the effect of pretreatment on carrageenan-induced paw edema, the following effects were measured 4 h post carrageenan injection. The data are given as mean \pm SEM (standard error of the mean), * $p < 0.05$, ** $p < 0.01$, *** $p < 0.001$ and ### indicates significant differences from the carrageenan-treated group.

The inhibitory potential of SF1–SF3 and SF13 was evaluated by measuring paw thickness (Table 7). The synthetic compounds showed a significant decrease in paw edema with time duration as compared to the standard, acetylsalicylic acid (ASA). The results revealed that the compounds showed

anti-inflammatory activity with meaningful statistical results. The results revealed that the compound with acetaminophen (**SF13**) significantly decreased the inflammation because of the acetaminophen moiety, which is categorized under non-steroidal anti-inflammatory drugs (NSAID) and has the potential to inhibit COX-1 and COX-2 enzymes involved in the production of prostaglandin [88]. Compounds **SF1**, **SF2** and **SF13**, with piperidine, morpholine and acetaminophen, also showed significant results in comparison to ASA.

Table 7. Effect of acute treatment of synthetic compounds (10 mg/kg) on carrageenan-induced inflammation ($n = 5$).

Compounds	Time After Carrageenan Injection ¹			
	0 h	2 h	4 h	6 h
Control	2.04 ± 0.07	2.05 ± 0.06	2.07 ± 0.04	2.10 ± 0.02
Carrageenan (100 µL)	2.11 ± 0.07	2.57 ± 0.08 ###	2.75 ± 0.07 ###	2.86 ± 0.05 ###
Acetyl salicylic acid (10 mg/kg)	2.14 ± 0.08	2.26 ± 0.05 ***	2.32 ± 0.04 ***	2.39 ± 0.02 ***
SF1 (10 mg/kg)	2.06 ± 0.07	2.13 ± 0.03 ***	2.18 ± 0.06 ***	2.25 ± 0.05 ***
SF2 (10 mg/kg)	2.05 ± 0.05	2.11 ± 0.06 ***	2.17 ± 0.03 ***	2.23 ± 0.07 ***
SF3 (10 mg/kg)	2.05 ± 0.06	2.16 ± 0.05 ***	2.22 ± 0.02 ***	2.28 ± 0.07 ***
SF13 (10 mg/kg)	2.04 ± 0.07	2.18 ± 0.03 ***	2.26 ± 0.06 ***	2.31 ± 0.07 ***

¹ Readings were measured every 2 h post carrageenan administration from 0 to 6 h. All values are expressed as mean ± SEM ($n = 5$). The data are given as mean ± SD, *** $p < 0.001$ and ### indicate significant differences from the carrageenan-treated group.

2.3.5. Structure-Activity Relationship (SAR)

The structure activity relationship is established from the findings of chemical moieties and their relationship to its biological activity. The results are summarized in Figure 10.

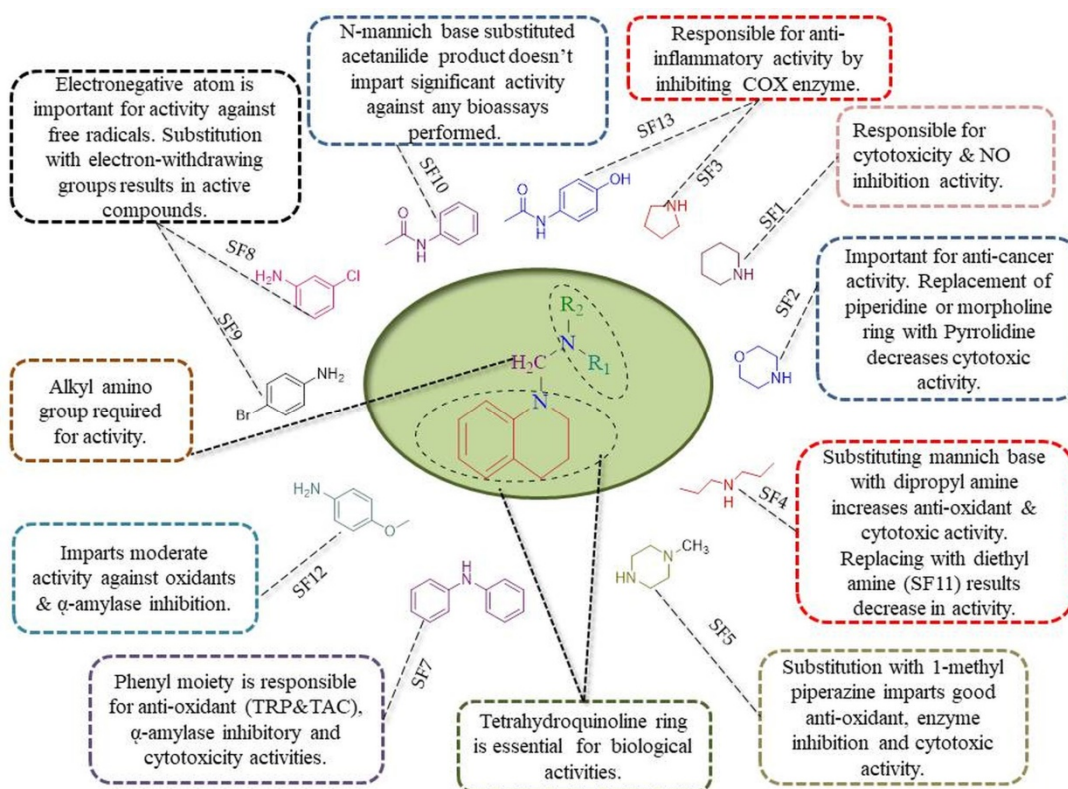


Figure 10. Structure–activity relationship of tetrahydroquinoline ring derivatized with thirteen amines.

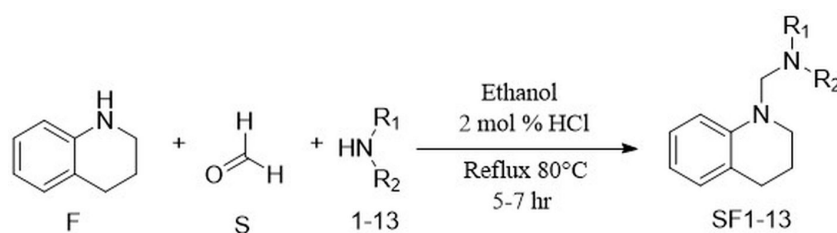
3. Materials and Methods

Unless otherwise noted, all commercially available compounds and solvents were purchased from Sigma-Aldrich and Merck, Germany. Analytical thin-layer chromatography (TLC) was performed with aluminum sheets, silica gel 60 F254 (Merck), by a solvent system, EtOAc: pentane in a 7:2 ratio and the products were visualized with UV irradiation (254 nm). Gallenkamp melting point apparatus was used to determine the melting points with open capillaries that are uncorrected. FTIR was recorded by the KBr pellets method by the PerkinElmer spectrum using the attenuated total reflectance (ATR). Nuclear magnetic resonance (NMR) spectra were recorded on an Agilent VNMR 400 (^1H NMR: 400 MHz, ^{13}C NMR: 101 MHz) or an Agilent VNMR 600 (^1H NMR: 600 MHz, ^{13}C NMR: 151 MHz) spectrometer. The chemical shifts are given in parts per million (ppm) relative to the residual solvent peak of the nondeuterated solvent (CDCl_3 ; ^1H NMR: $\delta = 7.26$ ppm; ^{13}C NMR: $\delta = 77.00$ ppm). The multiplicity was reported with the following abbreviations: s = singlet, d = doublet, t = triplet, m = multiplet, p = pentet, br = broad signal, dd = doublet of doublet, dt = doublet of triplet, ddt = doublet of doublet of triplet, td = triplet of doublet, tp = triplet of pentet, tdd = triplet of doublet of doublet. Mass spectra were recorded on a Finnigan SSQ 7000 spectrometer. The PE 2400 Series II CHNS/O Analyzer was used to determine the content of carbon, hydrogen and nitrogen in organic materials.

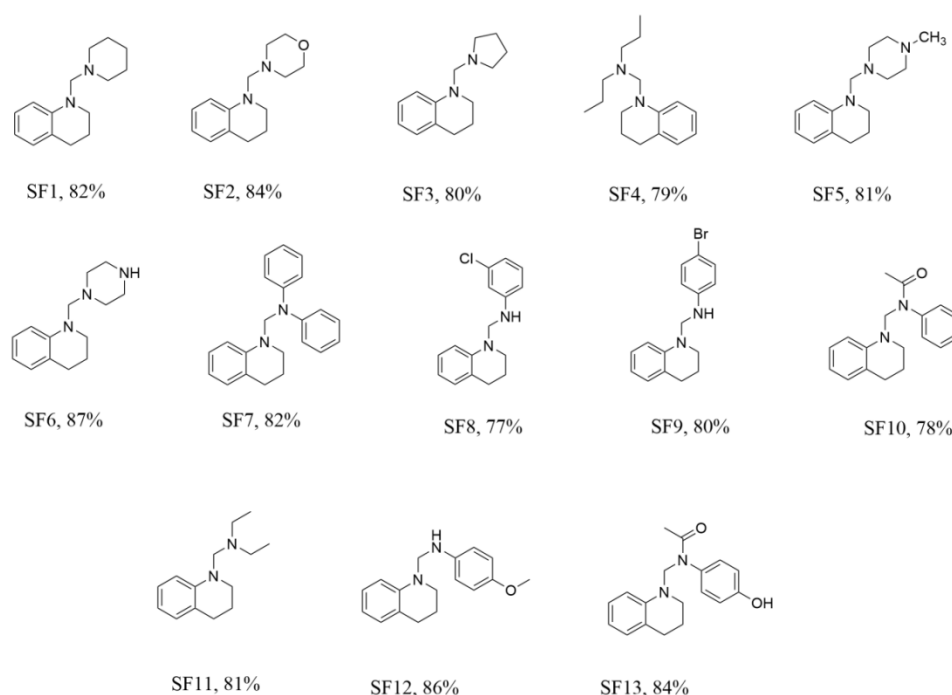
3.1. General Procedure for the Synthesis of N-Mannich Bases of Tetrahydroquinoline

In a pressure tube equipped with a stirring bar, amines **1–13** (1.0 equiv, 0.5 mmol), formaldehyde **S** (2.0 equiv, 1 mmol) and tetrahydroquinoline **F** (1.0 equiv, 0.5 mmol) were added into 3 mL of ethanol and the mixture was heated to 80 °C in an oil bath under reflux conditions. Concentrated HCl (2 mol %) was added as a catalyst. The reaction progress and completion of the reaction was monitored by TLC. After ~5–7 h of refluxing, the reaction mixture was removed and cooled at room temperature. The reaction mixture was neutralized with a NaHCO_3 solution and extracted with DCM (dichloromethane) (3×10 mL). The organic layer was dried over Na_2SO_4 and evaporated by a rotary evaporator. The product was washed and recrystallized by ethanol. For some of the compounds, an additional purification step of flash column chromatography was performed by using ethyl acetate: pentane in a 7:2 ratio.

The target compounds **SF1–SF13** were synthesized according to the synthetic route shown in Scheme 4.



Scheme 4. Cont.



Scheme 4. Synthesis of compounds **SF1–SF13**. Reaction conditions: **S** (2.0 equiv), **1–13** (1.0 equiv), **F** (1.0 equiv); 3 mL solvent, conc. HCl 2 mol %, 80 °C (oil bath). Yields obtained after purification of product.

1-(Piperidine-1-ylmethyl) 1, 2, 3, 4-tetrahydroquinoline (**SF1**)

White solid; yield 82%; m.p. 130–137 °C; $R_f = 0.89$; IR (ATR) ν_{max} 3397, 2850, 2327, 1710, 1613, 1437, 1191, 1042, 993 cm^{-1} ; $^1\text{H-NMR}$ (600 MHz, CDCl_3) δ ppm 6.94 (t, 1H), 6.91 (t, $J = 4.7$ Hz, 1H), 6.64 (dd, $J = 7.0, 3.7$ Hz, 1H), 6.60–6.54 (m, 1H), 4.70 (s, 2H), 3.27 (q, $J = 5.5$ Hz, 6H), 2.73 (t, 2H), 1.93 (td, $J = 5.3, 2.6$ Hz, 6H), 1.57 (t, 2H); $^{13}\text{C NMR}$ (151 MHz, CDCl_3) δ ppm 144.92, 127.11, 125.48, 63.50, 51.73, 47.07, 28.17, 25.92, 25.76, 22.35; EIMS m/z 230.2 (M+), Anal. ($\text{C}_{15}\text{H}_{22}\text{N}_2$): C 78.21, H 9.63, N 12.16, Calcd. C 78.27, H 9.61, N 12.19.

4-((3, 4-Dihydroquinolin-1(2H)-yl) methyl) morpholine (**SF2**)

Light yellow solid; yield 84%; m.p. 142–148 °C; $R_f = 0.63$; IR (ATR) ν_{max} 3390, 2834, 2322, 2083, 1898, 1663, 1611, 1503, 1304, 1049 cm^{-1} ; $^1\text{H NMR}$ (600 MHz, CDCl_3) δ ppm 7.04 (td, $J = 7.9, 7.4, 1.6$ Hz, 1H), 6.95 (dd, $J = 7.4, 1.5$ Hz, 1H), 6.88 (dd, $J = 8.3, 1.1$ Hz, 1H), 6.61 (td, $J = 7.3, 1.1$ Hz, 1H), 3.77 (s, 2H), 3.71 (t, 4H), 3.34 (t, 2H), 2.76 (t, $J = 6.4$ Hz, 2H), 2.50 (s, 4H), 1.93 (tt, 2H); $^{13}\text{C NMR}$ (151 MHz, CDCl_3) δ ppm 145.48, 129.03, 127.10, 126.88, 116.54, 67.01, 66.87, 52.00, 50.80, 27.94, 22.40; EIMS m/z 232 (M+), Anal. ($\text{C}_{14}\text{H}_{20}\text{N}_2\text{O}$): C 72.38, H 8.68, N 12.06, Calcd: C 72.39, H 8.67, N 12.08.

1-(Pyrrolidin-1-ylmethyl) -1, 2, 3, 4-tetrahydroquinoline (**SF3**)

Yellow solid; yield 80%; m.p. 115–117 °C; $R_f = 0.86$; IR (ATR) ν_{max} 3388, 2921, 2323, 1990, 1656, 1501, 1300, 1153, 972 cm^{-1} ; $^1\text{H NMR}$ (600 MHz, CDCl_3) δ ppm 7.03 (td, 1H), 6.94 (dd, 1H), 6.86 (td, 1H), 6.60 (dd, 1H), 3.98 (s, 2H), 2.77 (t, $J = 6.3$ Hz, 2H), 2.60 (ddt, $J = 6.7, 3.9, 2.1$ Hz, 5H), 1.95 (t, 2H), 1.79 (ddd, $J = 6.7, 4.6, 1.9$ Hz, 5H); $^{13}\text{C NMR}$ (151 MHz, CDCl_3) δ ppm 145.48, 129.05, 126.90, 122.17, 116.16, 67.48, 51.84, 26.97, 23.53, 22.41; EIMS m/z 216 (M+), Anal. ($\text{C}_{14}\text{H}_{20}\text{N}_2$): C 77.73, H 9.32, N 12.95, Calcd. C 77.77, H 9.31, N 12.97.

N-((3, 4-dihydroquinolin-1(2H)-yl), methyl)-N-propylpropan-1 amine (**SF4**)

Yellow powder; yield 79%; m.p. 123–132 °C; $R_f = 0.74$; IR (ATR) ν_{max} 3841, 2831, 1685, 1510, 1304, 972 cm^{-1} ; $^1\text{H NMR}$ (600 MHz, CDCl_3) δ ppm 6.98 (dd, 1H), 6.91 (td, 1H), 6.74 (dd, 1H), 6.66 (td, 1H),

4.71 (s, 2H), 3.29 (t, $J = 11.4$ Hz, 2H), 2.78–2.60 (m, 4H), 2.59 (t, 2H), 1.99–1.95 (m, 4H), 1.50 (t, 2H), 0.89 (tt, 6H); ^{13}C NMR (151 MHz, CDCl_3) δ ppm 145.95, 128.98, 127.17, 126.79, 122.44, 115.97, 67.48, 59.85, 46.94, 27.87, 22.41, 20.41, 11.82; EIMS m/z 246.22 (M+); Anal. ($\text{C}_{16}\text{H}_{26}\text{N}_2$): C 77.99, H 10.64, N 11.37, Found: C 77.95, H 10.67, N 11.39.

1-(4-Methylpiperazin-1-yl) methyl)-1, 2, 3, 4-tetrahydroquinoline (SF5)

Light yellow solid; yield 81%; m.p. 167 °C; $R_f = 0.76$; IR (ATR) ν_{max} 3354, 3061, 1605, 1461, 1354, 1003, 949 cm^{-1} ; ^1H NMR (600 MHz, CDCl_3) δ ppm 7.01–6.99 (m, 1H), 6.88 (td, $J = 7.5, 2.0$ Hz, 1H), 6.56 (td, $J = 7.5, 2.0$ Hz, 1H), 6.37 (dd, $J = 7.5, 2.0$ Hz, 1H), 4.42 (s, 2H), 3.33 (t, $J = 5.1$ Hz, 2H), 2.90 (td, $J = 6.2, 1.0$ Hz, 2H), 2.51–2.47 (m, 9H), 2.24 (s, 3H), 2.08–2.04 (m, 2H); ^{13}C NMR (151 MHz, CDCl_3) δ ppm 145.62, 128.98, 126.89, 122.28, 116.37, 67.47, 54.95, 50.29, 48.41, 46.08, 27.91, 22.42; EIMS m/z 245.20 (M+); Anal. ($\text{C}_{15}\text{H}_{23}\text{N}_3$): C 73.47, H 9.42, N 17.17, Found: C 73.43, H 9.45, N 17.13.

1-(Piperazine-1-yl methyl)-1, 2, 3, 4-tetrahydroquinoline (SF6)

Off-white crystals; yield 87%; m.p. 220–227 °C; $R_f = 0.77$; IR (ATR) ν_{max} 3863, 3379, 2833, 2493, 2285, 2088, 1900, 1655, 1611, 1500, 1314, 1050 cm^{-1} ; ^1H NMR (600 MHz, CDCl_3) δ ppm 6.97–6.94 (m, 2H), 6.59 (dd, $J = 7.4, 1.2$ Hz, 1H), 6.47 (d, $J = 1.1$ Hz, 1H), 3.81 (s, 2H), 3.30–3.29 (m, 4H), 2.94–2.85 (m, 4H), 2.76 (t, $J = 6.4$ Hz, 4H), 2.17 (s, 1H), 1.95–1.93 (m, 2H); ^{13}C NMR (151 MHz, CDCl_3) δ ppm 145.48, 129.03, 127.10, 126.88, 122.36, 116.54, 67.01, 52.00, 50.80, 46.93, 28.09, 22.21; EIMS m/z 231.34 (M+). Anal. ($\text{C}_{14}\text{H}_{21}\text{N}_3$): C 72.69, H 9.15, N 18.16, Found: C 72.66, H 9.19, N 18.21.

N-((3, 4-dihydroquinolin-1(2H)-yl) methyl)-N-phenylaniline (SF7)

Brown crystals; yield 82%; m.p. 243–248 °C; $R_f = 0.81$; IR (ATR) ν_{max} 3378, 2921, 2692, 2494, 2285, 2110, 1904, 1794, 1592, 1311, 1174, 946 cm^{-1} ; ^1H NMR (600 MHz, $\text{DMSO}-d_6$) δ ppm 7.24–7.20 (m, 8H), 7.05–6.99 (m, 3H), 6.88 (td, $J = 7.5, 2.0$ Hz, 1H), 6.56 (td, $J = 7.5, 2.0$ Hz, 1H), 6.38 (dd, $J = 7.5, 2.0$ Hz, 1H), 5.12 (s, 2H), 3.33 (t, $J = 5.1$ Hz, 2H), 2.90 (td, $J = 6.3, 1.1$ Hz, 2H), 2.06 (tt, $J = 6.2, 5.1$ Hz, 2H); ^{13}C NMR (151 MHz, $\text{DMSO}-d_6$) δ ppm 148.27, 129.32, 129.26, 129.13, 122.46, 122.22, 121.49, 121.45, 120.95, 120.68, 117.76, 111.17, 111.04, 89.72, 62.07, 55.77, 54.85, 51.42, 49.45, 40.02, 22.48, 22.38; EIMS m/z 314 (M+); Anal. ($\text{C}_{22}\text{H}_{22}\text{N}_2$): C 84.04, H 7.05, N 8.91, Found: C 83.07, H 7.07, N 8.91.

3-Chloro-N-((3, 4-dihydroquinolin-1(2H)-yl) methyl) aniline (SF8)

Brown solid; yield 77%; m.p. 219 °C; $R_f = 0.83$; IR (KBr) ν_{max} 3357, 2921, 2835, 2287, 2113, 1795, 1598, 1314, 1197, 989 cm^{-1} ; ^1H NMR (600 MHz, $\text{DMSO}-d_6$) δ ppm 7.09–7.03 (m, $J = 27.7, 6.8$ Hz, 3H), 7.01–6.96 (m, 2H), 6.74 (s, 1H), 6.69–6.65 (dd, 1H), 6.54 (d, $J = 2.9$ Hz, 1H), 4.70 (s, 2H), 4.35 (s, 1H), 3.40 (t, 2H), 2.80 (d, $J = 12.5$ Hz, 2H), 2.01–1.97 (m, 2H); ^{13}C NMR (151 MHz, $\text{DMSO}-d_6$) δ ppm 147.67, 134.84, 130.66, 127.57, 127.27, 124.27, 121.23, 115.97, 115.36, 114.92, 114.20, 58.76, 48.77, 27.00, 22.40; EIMS m/z 272.78 (M+). Anal. ($\text{C}_{16}\text{H}_{17}\text{ClN}_2$) C 70.45, H 6.28, N 10.27, Found: C 70.49, H 6.23, N 10.28.

4-Bromo-N-((3, 4-dihydroquinolin-1(2H)-yl) methyl) aniline (SF9)

Green solid; yield 80%; m.p. 200 °C; $R_f = 0.81$; IR (ATR) ν_{max} 3631, 2834, 2287, 1902, 1612, 1313, 1194, 1070, 944 cm^{-1} ; ^1H NMR (600 MHz, $\text{DMSO}-d_6$) δ ppm 7.24–7.22 (m, 2H), 7.00 (ddt, $J = 7.5, 2.0, 0.9$ Hz, 1H), 6.88 (td, $J = 7.5, 2.0$ Hz, 1H), 6.67–6.65 (m, 2H), 6.56 (td, $J = 7.5, 2.0$ Hz, 1H), 6.38 (dd, $J = 7.5, 2.0$ Hz, 1H), 5.12 (s, 2H), 3.43 (s, 1H), 3.33 (t, $J = 5.2$ Hz, 2H), 2.90 (td, $J = 6.1, 1.0$ Hz, 2H), 2.06 (tt, $J = 6.1, 5.2$ Hz, 2H); ^{13}C NMR (151 MHz, $\text{DMSO}-d_6$) δ ppm 147.42, 144.96, 132.16, 127.52, 127.14, 124.22, 122.56, 119.33, 115.06, 114.31, 111.50, 61.78, 48.79, 26.98, 22.38; EIMS m/z 316 (M+). Anal. ($\text{C}_{16}\text{H}_{17}\text{BrN}_2$) C 60.58, H 5.40, N 8.83, Found: C 60.54, H 5.42, N 8.86.

N-((3, 4-dihydroquinolin-1(2H)-yl) methyl)-N-phenylacetamide (SF10)

White crystals; yield 78%; m.p. 220 °C; $R_f = 0.93$; IR (ATR) ν_{max} 3863, 3371, 2931, 2689, 2326, 2110, 1906, 1661, 1598, 1372, 1073, 884 cm^{-1} ; ^1H NMR (600 MHz, CDCl_3) δ ppm 7.49–7.47 (m, 2H), 7.37–7.28 (m, 3H), 7.00 (ddt, $J = 7.5, 2.0, 1.0$ Hz, 1H), 6.88 (td, $J = 7.5, 2.0$ Hz, 1H), 6.56 (td, $J = 7.5, 2.0$ Hz, 1H),

6.38 (dd, $J = 7.5, 2.0$ Hz, 1H), 5.44 (s, 2H), 3.33 (t, $J = 5.1$ Hz, 2H), 2.90 (td, $J = 6.2, 1.0$ Hz, 2H), 2.08–2.04 (m, 2H), 2.05 (s, 3H); ^{13}C NMR (151 MHz, CDCl_3) δ ppm 168.68, 142.24, 137.99, 128.92, 128.22, 128.11, 127.22, 125.55, 124.24, 119.97, 117.44, 49.53, 27.74, 22.57, 22.46; EIMS m/z 280 (M+). Anald. ($\text{C}_{18}\text{H}_{20}\text{N}_2\text{O}$) C 77.11, H 7.19, N 9.99, Found: C 77.13, H 7.19, N 9.96.

N-((3, 4-dihydroquinolin-1(2H)-yl) methyl)-*N*-ethylethanamine (SF11)

Off-white solid; yield 81%; m.p. 110 °C; $R_f = 0.86$; IR (ATR) ν_{max} 3851, 3373, 2838, 2235, 2003, 1895, 1610, 1496, 1198, 1093 cm^{-1} ; ^1H NMR (400 MHz, CDCl_3) δ ppm 6.99–6.95 (dd, $J = 8.2, 1.6$ Hz, 1H), 6.93–6.87 (m, 1H), 6.85–6.80 (m, 1H), 6.53 (dt, $J = 23.3, 7.3, 1.2$ Hz, 1H), 3.81 (s, 2H), 3.26–3.18 (m, 2H), 2.69 (td, 2H), 2.60–2.47 (m, 4H), 1.86 (tt, 2H), 0.99–0.92 (m, 6H); ^{13}C NMR (101 MHz, CDCl_3) δ ppm 145.93, 129.04, 127.14, 126.88, 122.46, 116.09, 46.98, 27.00, 22.46, 11.88; EIMS m/z 218 (M+). Anald. ($\text{C}_{14}\text{H}_{22}\text{N}_2$) C 77.01, H 10.16, N 12.83, Found: C 77.04, H 10.13, N 12.83.

N-((3, 4-dihydroquinolin-1(2H)-yl) methyl)-4-methoxyaniline (SF12)

Pale yellow solid; yield 86%; m.p. 215 °C; $R_f = 0.78$; IR (ATR) ν_{max} 3853, 3393, 2997, 2833, 2323, 2160, 2077, 1887, 1611, 1305, 1154, 1036, 975 cm^{-1} ; ^1H NMR (600 MHz, CDCl_3) δ ppm 6.97–6.87 (m, 4H), 6.73 (dd, $J = 17.1, 9.0$ Hz, 2H), 6.65 (dd, $J = 8.4, 1.1$ Hz, 1H), 6.54 (td, 1H), 4.60 (s, 2H), 4.32 (s, 1H), 3.67 (s, 3H), 3.21 (td, 2H), 2.69 (s, 1H), 1.87–1.84 (m, 2H); ^{13}C NMR (151 MHz, CDCl_3) δ ppm 154.07, 144.97, 143.67, 128.92, 127.31, 124.21, 122.18, 120.93, 120.09, 114.47, 55.77, 55.56, 46.97, 26.98, 22.39; EIMS m/z 269 (M+). Anald. ($\text{C}_{17}\text{H}_{20}\text{N}_2\text{O}$) C 76.09, H 7.51, N 10.54, Found: C 76.07, H 7.53, N 10.54.

N-((3, 4-dihydroquinolin-1(2H)-yl) methyl)-*N*-(4-hydroxyphenyl) acetamide (SF13)

White solid; yield 84%; m.p. 285 °C; $R_f = 0.91$; IR (ATR) ν_{max} 3249, 2831, 2611, 2063, 1893, 1611, 1454, 1370, 1233, 1019, 833 cm^{-1} ; ^1H NMR (400 MHz, $\text{DMSO}-d_6$) δ ppm 9.95 (s, 1H), 7.08–7.06 (m, 2H), 7.00 (ddt, $J = 7.5, 2.0, 1.0$ Hz, 1H), 6.88 (td, $J = 7.5, 2.0$ Hz, 1H), 6.72–6.69 (m, 2H), 6.56 (td, $J = 7.5, 2.0$ Hz, 1H), 6.38 (dd, $J = 7.5, 2.0$ Hz, 1H), 5.44 (s, 2H), 3.33 (t, $J = 5.2$ Hz, 2H), 2.90 (td, $J = 6.0, 1.0$ Hz, 2H), 2.06 (tt, $J = 6.0, 5.2$ Hz, 2H), 2.03 (s, 3H); ^{13}C NMR (101 MHz, $\text{DMSO}-d_6$) δ ppm 168.58, 153.46, 145.77, 130.06, 128.73, 127.15, 127.12, 125.40, 120.95, 115.54, 88.78, 49.27, 27.49, 22.64, 22.39; EIMS m/z 296 (M+); Anald. ($\text{C}_{18}\text{H}_{20}\text{N}_2\text{O}_2$) C 72.95, H 6.80, N 9.45, Found: C 72.93, H 6.82, N 9.44.

Figures S1–S26 (Supplementary Materials) report the ^1H and ^{13}C -NMR spectra of all the synthesized compounds.

3.2. ADME Predictions

A computational study to predict the ADME (absorption, distribution, metabolism, excretion) properties of the synthesized compounds (SF1–SF13) was performed using SwissADME software [89] to determine drug-likeness properties. We determined the following parameters: molecular weight (MW), molar refractivity logarithm of the partition coefficient (ilog $P_{\text{O/W}}$), Alog P, HBA and HBD to forecast Lipinski's rule of five (RO5).

3.3. Bioevaluation

3.3.1. Antioxidant Assay

DPPH Assay

The % FRSA (free radical scavenging activity) of the synthetic compounds was determined by using the method of Tai et al. [90] with slight modifications. The antioxidant potential was determined by detecting the capacity of the synthetic compounds to quench the DPPH free radicals. The synthetic compounds were taken in a 96-well plate at three-fold concentrations of 200 $\mu\text{g/mL}$, 66.6 $\mu\text{g/mL}$, 22.2 $\mu\text{g/mL}$ and 7.4 $\mu\text{g/mL}$. DPPH free radicals were added to entire wells to make up the volume up to 200 μL . DMSO and ascorbic acid were taken as negative and positive controls, respectively.

The absorbance was taken at 630nm using a microplate reader (ELx800 BioTek). The percentage of scavenging activity was calculated by the given formula:

$$\% \text{ scavenging activity} = (1 - Ab_s/Ab_c) \times 100$$

Abs = sample's absorbance; Abc = control's absorbance.

Determination of Total Antioxidant Capacity (TAC)

The total antioxidant capacity was determined by using the phosphomolybdenum-based method [91]. The method is based on the reduction of Mo (VI) to Mo (V), leading to the formation of a green-colored phosphate–molybdenum complex that gives absorption at 630 nm. In 96-well plates, 20 μ L of the sample was added with 180 μ L TAC reagents in it and incubated at 95 °C for 90 min in a water bath and cooled at room temperature. The results were calculated as μ g AAE/mg.

Total Reducing Power (TRP) Determination

The assay is based on the reduction of Fe^{+3} to Fe^{+2} . The method described by Khan et al. was used with slight modifications. One hundred microliters of test samples (4 mg/mL DMSO) were taken in an Eppendorf tube and 200 μ L of phosphate buffer (0.2 mol/L, pH 6.6) and 250 μ L of 1% potassium ferricyanide ($K_3Fe(CN)_6$) were added. This was allowed to incubate at 50 °C for 20 min. Later on, 200 μ L of 10% trichloroacetic acid (TCA) was added to the mixture. The mixture was centrifuged at 3000 rpm at room temperature for 10 min. After centrifugation, 150 μ L of supernatant were transferred to microplate with $FeCl_3$ (50 μ L, 0.1%) and the absorbance was taken at 630 nm [92]. The results were calculated as μ g AAE/mg.

3.3.2. α -Amylase Enzyme Inhibitory Assay

An in vitro α -amylase enzyme inhibitory assay was performed by the standard protocol [93]. Four milligrams per 1 mL of sample was prepared in DMSO. In each well of a 96-well plate, synthetic compounds were added to a final concentration of 200 μ g/mL. To this, 15 μ L phosphate buffer, 25 mL α -amylase enzyme and 40 μ L starch solution were added stepwise. The microplate was incubated at 50 °C for 30 min. Twenty microliters of HCl (1 M) and 90 μ L iodine solution (0.254 g I_2 and 4 g of KI in 1 L of distilled water) were added and the reading was noted at 540 nm. Acarbose and DMSO were taken as positive and negative controls, respectively. The formula used to calculate the percent enzyme inhibition is:

$$\% \text{ Enzyme inhibition} = [(As - An) \div (Ab - An)] \times 100$$

As = sample's absorbance; An = negative's absorbance; Ab = blank's absorbance

Synthetic compounds with a % enzyme inhibition \geq 50% were taken at three-fold concentrations of 200 μ g/mL, 66.6 μ g/mL, 22.2 μ g/mL and 7.4 μ g/mL and their IC_{50} was calculated.

3.4. Cytotoxicity Evaluation

Brine Shrimp Cytotoxicity Assay

Brine shrimp eggs were hatched in a shallow rectangular plastic dish and filled with artificial seawater, which was prepared with a commercial salt mixture. In a 96-well plate, 150 μ L of artificial seawater was added and 10 nauplii were added into this. Test compounds (400, 200, 100 and 50 μ g/mL) were added into each well and the final volume was made up by adding the artificial seawater. The well plate was left uncovered under a lamp. The number of surviving shrimps were counted and recorded after 24 h. The test was repeated in triplicate [94]. Using GraphPad Prism, the lethality concentration (LD_{50}) was assessed at 95% confidence intervals. The percentage mortality (%M) was also calculated by dividing the number of dead nauplii by the total number and then multiplied by 100.

Cytotoxicity Against Raw Macrophages

The cytotoxic potential was assessed by using an MTT 3-(4,5-dimethyl thiazole-2-yl)-2,5-diphenyl tetrazolium bromide assay [95]. Briefly, macrophages were extracted from the peritoneal cavity of albino rats and plated at a density of 1×10^6 per well in a 96-well plate and incubated in a 5% CO₂ incubator at 37 °C for 24 h. The cells were treated with various concentrations of the test compounds (100 µM, 50 µM, 10 µM and 1 µM) or vehicle alone. The test compounds were first dissolved in DMSO to make a 100 mM stock solution and then further dilutions were made from this stock solution. After 24 h of incubation, 20 µL of MTT (1 mg/mL in normal saline) was added into each well and incubated under the same conditions for 2 h. Mitochondrial succinate dehydrogenase converted MTT in live cells into purple formazan crystals. The formazan crystals were then solubilized in 100 µL DMSO, and the absorbance was measured at 570 nm. The % cell viability was calculated by the following formula;

$$\% \text{ cell viability} = (\text{abs}_{\text{sample}} - \text{abs}_{\text{blank}}) / (\text{abs}_{\text{control}} - \text{abs}_{\text{blank}}) \times 100$$

MTT Assay Against Hep-2C Cells

Hep-2C cell line experiments were performed in the Immunology Lab of the National Institute of Health (NIH), Islamabad, Pakistan. Human cervix carcinoma cells Hep-2C (ATCC HB-8065) were cultured in Dulbecco's modified Eagle's medium (DMEM), comprising 10% fetal calf serum (10% FCS) and supplemented with 2 mM L-glutamine, 100 U/mL penicillin, 100 µg/mL streptomycin and 1 mM Na pyruvate, at 37 °C in a humidified 5% CO₂ incubator.

The tetrazolium dye 3-(4, 5-dimethyl thiazolyl-2)-2, 5-diphenyltetrazolium bromide (MTT) was used to assess the cytotoxic potential of the test compounds. In living cells, MTT is reduced into its insoluble purple product formazan, which is measured spectrophotometrically.

Hep-2C cells, in a density of 1×10^6 (> 90% cell viability), were cultured in a 96-well plate and treated with different concentrations of the test compounds for 24, 48 and 72 h. Ten microliters of MTT (1 mg per mL) were added per well followed by incubation for 4 h. Insoluble formazan crystals were dissolved by adding 100 µL of DMSO. Cells were then incubated for another 2 h. Absorbance was measured at 570 nm by a microplate reader [96]. Untreated Hep-2C cells were taken as controls and DMSO as a negative.

$$\% \text{ cell viability} = (\text{abs}_{\text{sample}} - \text{abs}_{\text{blank}}) / (\text{abs}_{\text{control}} - \text{abs}_{\text{blank}}) \times 100$$

3.5. Nitric Oxide Assay

Isolation of Peritoneal Macrophages and Measurement of Nitrite Production

The anti-inflammatory effect of the synthesized compounds in murine macrophages was evaluated by using the Griess reaction method, described previously [97]. In brief, 1×10^6 were plated in a 96-well plate and incubated in a 5% CO₂ incubator at 37 °C for 24 h, pre-treated with different concentrations (100 µM, 50 µM, 10 µM and 1 µM) of synthetic compounds for another 2 h and challenged with LPS (1 µg/mL) for an additional 18 h. Equal volumes of Griess reagent (1% sulphanilamide in 50% phosphoric acid and 0.1% naphthyl ethylenediamine dihydrochloride in distilled water and vortexed) and culture medium were mixed and the absorbance was taken at 540 nm. Lipopolysaccharide (LPS) was taken as a blank and piroxicam was taken as a positive control. A *t*-test was applied to determine the significance of the results.

In Vivo Anti-Inflammatory Activity

At 7–8 weeks old, male BALB/C albino mice (29–35 g), were purchased from The National Institute of Health (NIH), Islamabad, Pakistan. Five animals were housed per group and placed in a controlled temperature and humidity-controlled room (22 °C and 66 ± 5%, respectively) in a 12 h light–dark cycle and provided with water and food ad libitum. Ethical approval was taken from the bio-ethical

committee of Quaid-I-Azam University (Approval No. BEC-FBS-QAU2018-119) and all protocols were conducted following the Ethical Guide to the Code of Practice for the Housing and Care of Animals Act 1986 (ARRIVE (Animal Research: Reporting In Vivo Experiments) guidelines).

The anti-inflammatory activity of the synthesized compounds was evaluated by using the carrageenan-induced rat paw edema assay. To determine the dose response of tetrahydroquinoline derivatives, animals were first given a dose of 0.1, 1 and 10 mg/kg against 100 μ L carrageenan (1% solution in normal saline)/paw. Treatment was given 60 min before carrageenan injection. Readings were taken at 4 h post carrageenan injection [98].

The in vivo anti-inflammatory activity was performed following the procedure described by Koksai, et al. [85] in 2017. Paw edema was induced by injecting 100 μ L of 1% sterile carrageenan solution into the right hind paw of mice. Synthesized compounds (10 mg/kg), vehicle (saline with 2% DMSO) and drug (acetylsalicylic acid, ASA 10 mg/kg) were administered to the mice orally by gastric intubation 60 min before injecting carrageenan into the right hind paw. The decrease in edema was measured by vernier calipers every 2 h.

3.6. Statistical Analysis

The experimental results were expressed as mean \pm SEM. Each test was performed in triplicate. The results were statistically analyzed by *t*-tests and ANOVA at a 95% confidence level ($p < 0.05$). GraphPad Prism software was used to calculate the half maximal inhibitory concentration (IC₅₀). A value of $p < 0.05$ was chosen as the criterion for statistical significance.

4. Conclusions

A series of N-Mannich bases, containing a tetrahydroquinoline nucleus, were synthesized and evaluated biologically for their drug-likeness properties, antioxidant potential, α -amylase enzyme inhibition, cytotoxicity and in vivo anti-inflammatory properties. The results of these assays were found to be encouraging and promising. The compounds exhibited significant scavenging DPPH free radical activity, i.e., **SF8** had the lowest IC₅₀ = 29.19 \pm 0.29 μ g/mL and **SF5** was the most potent in inhibiting α -amylase enzyme, i.e., 97.47%. The compounds were successfully evaluated for their cytotoxic activities on the raw macrophages and anti-tumor activity using the cervix carcinoma cell line (Hep-2C). Compounds **SF1** and **SF7** revealed cytotoxicity to the cervix carcinoma cell line. These results revealed that the cytotoxic potential of new compounds can be a starting point for further surveying them as chemotherapeutic agents in cancer treatment. Moreover, the compounds were further tested on animal models to evaluate their anti-inflammatory behavior. Moderate to potent anti-inflammatory activity of these derivatives containing tetrahydroquinoline was observed, which is comparable with the standard drug, acetylsalicylic acid. As a conclusion, the current study gave us the scope for further work in this area for future developments through derivatization to design more potent compounds. It felt necessary from the results of the current work that there is a need for further advanced studies, at least on the few synthetic compounds which are found to be superior and to produce a rational quantitative structure–activity relationship (QSAR) mapping.

Supplementary Materials: The following are available online at <http://www.mdpi.com/1420-3049/25/11/2710/s1>, Figure S1–S26 represent the ¹H NMR and ¹³C NMR of the synthetic compounds.

Author Contributions: Funding acquisition, S.F.; methodology, S.F., A.M. and A.G.; resources, I.-U.-H.; supervision, N.U.; writing—original draft, S.F.; writing—review and editing, S.F., N.U. and I.-U.-H. All authors have read and agreed to the published version of the manuscript.

Funding: This research was funded by the Higher Education Commission (HEC) of Pakistan, grant number, PIN NO. 315-11229-2MD3-036.

Acknowledgments: Samra Farooq was financially supported by the Indigenous Ph.D. scholarship (PIN NO. 315-11229-2MD3-036) granted by the Higher Education Commission (HEC) of Pakistan. We are grateful to the National Institute of Health (NIH) for providing Hep-2C cell lines. The authors acknowledge Prof. Carsten Bolm (RWTH Aachen University, Germany) for the equipment and assistance with the acquisition of the characterization analysis.

Conflicts of Interest: The authors declare that there was no conflict of interest and are responsible for the content and writing of the paper.

Abbreviations

The following abbreviations are used in this manuscript.

THQ	Tetrahydroquinoline
ASA	Acetylsalicylic acid
FRSA	Free radical scavenging activity
TAC	Total antioxidant capacity
TRP	Total reducing power
NO	Nitric oxide
SEM	Standard error of the mean
SD	Standard deviation
DMSO	Dimethylsulfoxide
KBr	Potassium bromide
DM	Diabetes mellitus
ROS	Reactive oxygen species
COX-I/II	Cyclooxygenase I/II
MCR	Multicomponent reaction
CDCl ₃	Deuterated chloroform
ADME	Absorption, distribution, metabolism, excretion
AAE	Ascorbic acid equivalent
LD	Lethal dose
TLC	Thin-layer chromatography
DCM	Dichloromethane
SAR	Structure–activity relationship
RO5	Rule of five (Lipinski’s five pints)
MTT	3-(4,5-Dimethylthiazol-2-yl)-2,5-diphenyl tetrazolium bromide
DPPH	2, 2-Diphenyl-1-picrylhydrazine

References

1. Patwardhan, B.; Vaidya, A.D.; Chorghade, M.; Joshi, S.P. Reverse pharmacology and systems approaches for drug discovery and development. *Curr. Bioact. Compd.* **2008**, *4*, 201–212. [[CrossRef](#)]
2. Campos, K.R.; Coleman, P.J.; Alvarez, J.C.; Dreher, S.D.; Garbaccio, R.M.; Terrett, N.K.; Tillyer, R.D.; Truppo, M.D.; Parmee, E.R. The importance of synthetic chemistry in the pharmaceutical industry. *Science* **2019**, *363*, eaat0805. [[CrossRef](#)]
3. Afsah, E.M.; Fadda, A.A.; Hammouda, M.M. Synthesis and antioxidant activity of 2-indolinone bis (Mannich bases) and related compounds. *Mon. Chem. Chem. Mon.* **2016**, *147*, 2009–2016. [[CrossRef](#)]
4. Kattappagari, K.K.; Teja, C.R.; Kommalapati, R.K.; Poosarla, C.; Gontu, S.R.; Reddy, B.V.R. Role of antioxidants in facilitating the body functions: A review. *J. Orof. Sci.* **2015**, *7*, 71. [[CrossRef](#)]
5. Garcia, E.J.; Oldoni, T.L.C.; Alencar, S.M.d.; Reis, A.; Loguercio, A.D.; Grande, R.H.M. Antioxidant activity by DPPH assay of potential solutions to be applied on bleached teeth. *Braz. Dent. J.* **2012**, *23*, 22–27. [[CrossRef](#)]
6. Demirci, S.; Demirbaş, N. Anticancer activities of novel Mannich bases against prostate cancer cells. *Med. Chem. Res.* **2019**, *28*, 1945–1958. [[CrossRef](#)]
7. Aschner, P. Current concepts of diabetes mellitus. *Int. Ophthalmol. Clin.* **1998**, *38*, 1–10. [[CrossRef](#)]
8. Sõukand, R.; Pieroni, A.; Biró, M.; Dénes, A.; Dogan, Y.; Hajdari, A.; Kalle, R.; Reade, B.; Mustafa, B.; Nedelcheva, A. An ethnobotanical perspective on traditional fermented plant foods and beverages in Eastern Europe. *J. Ethnopharmacol.* **2015**, *170*, 284–296. [[CrossRef](#)]
9. Etxeberria, U.; de la Garza, A.L.; Campión, J.; Martínez, J.A.; Milagro, F.I. Antidiabetic effects of natural plant extracts via inhibition of carbohydrate hydrolysis enzymes with emphasis on pancreatic alpha amylase. *Expert Opin. Ther. Targets* **2012**, *16*, 269–297. [[CrossRef](#)]

10. Balan, K.; Ratha, P.; Prakash, G.; Viswanathamurthi, P.; Adisakwattana, S.; Palvannan, T. Evaluation of invitro α -amylase and α -glucosidase inhibitory potential of N2O2 schiff base Zn complex. *Arab. J. Chem.* **2017**, *10*, 732–738. [[CrossRef](#)]
11. Arora, R.K.; Kaur, N.; Bansal, Y.; Bansal, G. Novel coumarin–benzimidazole derivatives as antioxidants and safer anti-inflammatory agents. *Acta Pharm. Sin. B* **2014**, *4*, 368–375. [[CrossRef](#)]
12. Madar, J.M.; Shastri, L.A.; Shastri, S.L.; Holiyachi, M.; Naik, N.; Kulkarni, R.; Shaikh, F.; Sungar, V. Design, synthesis, characterization, and biological evaluation of pyrido [1, 2-a] pyrimidinone coumarins as promising anti-inflammatory agents. *Synth. Commun.* **2018**, *48*, 375–386. [[CrossRef](#)]
13. Yin, L.-L.; Zhang, W.-Y.; Li, M.-H.; Shen, J.-K.; Zhu, X.-Z. CC05, a novel anti-inflammatory compound, exerts its effect by inhibition of cyclooxygenase-2 activity. *Eur. J. Pharmacol.* **2005**, *520*, 172–178. [[CrossRef](#)]
14. Zhang, X.; Cao, J.; Zhong, L. Hydroxytyrosol inhibits pro-inflammatory cytokines, iNOS, and COX-2 expression in human monocytic cells. *Naunyn-Schmiedebergs Arch. Pharmacol.* **2009**, *379*, 581. [[CrossRef](#)]
15. Hseu, Y.-C.; Wu, F.-Y.; Wu, J.-J.; Chen, J.-Y.; Chang, W.-H.; Lu, F.-J.; Lai, Y.-C.; Yang, H.-L. Anti-inflammatory potential of Antrodia camphorata through inhibition of iNOS, COX-2 and cytokines via the NF- κ B pathway. *Int. Immunopharmacol.* **2005**, *5*, 1914–1925. [[CrossRef](#)]
16. Sharma, J.; Al-Omran, A.; Parvathy, S. Role of nitric oxide in inflammatory diseases. *Inflammopharmacology* **2007**, *15*, 252–259. [[CrossRef](#)]
17. Bogdan, C. Nitric oxide and the immune response. *Nat. Immunol.* **2001**, *2*, 907–916. [[CrossRef](#)]
18. Aktan, F. iNOS-mediated nitric oxide production and its regulation. *Life Sci.* **2004**, *75*, 639–653. [[CrossRef](#)]
19. Insuasty, D.; Castillo, J.; Becerra, D.; Rojas, H.; Abonia, R. Synthesis of Biologically Active Molecules through Multicomponent Reactions. *Molecules* **2020**, *25*, 505. [[CrossRef](#)]
20. Cioc, R.C.; Ruijter, E.; Orru, R.V. Multicomponent reactions: Advanced tools for sustainable organic synthesis. *Green Chem.* **2014**, *16*, 2958–2975. [[CrossRef](#)]
21. Fields, E.K. The synthesis of esters of substituted amino phosphonic acids1a. *J. Am. Chem. Soc.* **1952**, *74*, 1528–1531. [[CrossRef](#)]
22. Lal, J.; Gupta, S.K.; Thavaselvam, D.; Agarwal, D.D. Synthesis and pharmacological activity evaluation of curcumin derivatives. *Chin. Chem. Lett.* **2016**, *27*, 1067–1072. [[CrossRef](#)]
23. Dayal, N.; Mikek, C.G.; Hernandez, D.; Naclerio, G.A.; Chu, E.F.Y.; Carter-Cooper, B.A.; Lapidus, R.G.; Sintim, H.O. Potently inhibiting cancer cell migration with novel 3H-pyrazolo [4, 3-f] quinoline boronic acid ROCK inhibitors. *Eur. J. Med. Chem.* **2019**, *180*, 449–456. [[CrossRef](#)]
24. Tenti, G.; Parada, E.; León, R.; Egea, J.; Martínez-Revelles, S.; Briones, A.M.; Sridharan, V.; López, M.G.; Ramos, M.T.; Menéndez, J.C. New 5-unsubstituted dihydropyridines with improved CaV1. 3 selectivity as potential neuroprotective agents against ischemic injury. *J. Med. Chem.* **2014**, *57*, 4313–4323. [[CrossRef](#)]
25. Pourshojaei, Y.; Abiri, A.; Eskandari, R.; Dourandish, F.; Eskandari, K.; Asadipo, A. Synthesis, biological evaluation, and computational studies of novel fused six-membered O-containing heterocycles as potential acetylcholinesterase inhibitors. *Comput. Biol. Chem.* **2019**, *80*, 249–258. [[CrossRef](#)]
26. Lakshmi, N.V.; Thirumurugan, P.; Noorulla, K.; Perumal, P.T. InCl₃ mediated one-pot multicomponent synthesis, anti-microbial, antioxidant and anticancer evaluation of 3-pyranyl indole derivatives. *Bioorg. Med. Chem. Lett.* **2010**, *20*, 5054–5061. [[CrossRef](#)]
27. Murlykina, M.V.; Sakhno, Y.I.; Desenko, S.M.; Konovalova, I.S.; Shishkin, O.V.; Sysoiev, D.A.; Kornet, M.N.; Chebanov, V.A. Features of switchable multicomponent heterocyclizations of salicylic aldehydes and 5-aminopyrazoles with pyruvic acids and antimicrobial activity of the reaction products. *Tetrahedron* **2013**, *69*, 9261–9269. [[CrossRef](#)]
28. Darandale, S.N.; Pansare, D.N.; Mulla, N.A.; Shinde, D.B. Green synthesis of tetrahydropyrimidine analogues and evaluation of their antimicrobial activity. *Bioorg. Med. Chem. Lett.* **2013**, *23*, 2632–2635. [[CrossRef](#)]
29. Aouali, M.; Mhalla, D.; Allouche, F.; El Kaim, L.; Tounsi, S.; Trigui, M.; Chabchoub, F. Synthesis, antimicrobial and antioxidant activities of imidazotriazoles and new multicomponent reaction toward 5-amino-1-phenyl [1, 2, 4] triazole derivatives. *Med. Chem. Res.* **2015**, *24*, 2732–2741. [[CrossRef](#)]
30. Kenchappa, R.; Bodke, Y.D.; Chandrashekar, A.; Telkar, S.; Manjunatha, K.; Sindhe, M.A. Synthesis of some 2, 6-bis (1-coumarin-2-yl)-4-(4-substituted phenyl) pyridine derivatives as potent biological agents. *Arab. J. Chem.* **2017**, *10*, S1336–S1344. [[CrossRef](#)]

31. Ezzatzadeh, E.; Hossaini, Z.; Varasteh Moradi, A.; Salimifard, M.; Afshari-Sharif Abad, S. Copper iodide and ZnO nanoparticles catalyzed multicomponent synthesis of 1, 3-cyclopentadiene: Study of antioxidant activity. *Can. J. Chem.* **2019**, *97*, 270–276. [[CrossRef](#)]
32. Kouznetsov, V.V.; Puentes, C.O.; Bohorquez, A.R.; Zacchino, S.A.; Sortino, M.; Gupta, M.; Vazquez, Y.; Bahsas, A.; Amaro-Luis, J. A straightforward synthetic approach to antitumoral pyridinyl substituted 7H-indeno [2, 1-c] quinoline derivatives via three-component imino Diels-Alder reaction. *Lett. Org. Chem.* **2006**, *3*, 300–304. [[CrossRef](#)]
33. Roopan, S.M.; Khan, F.N.; Jin, J.S.; Kumar, R.S. An efficient one pot–three component cyclocondensation in the synthesis of 2-(2-chloroquinolin-3-yl)-2, 3-dihydroquinazolin-4 (1H)-ones: Potential antitumor agents. *Res. Chem. Intermed.* **2011**, *37*, 919. [[CrossRef](#)]
34. Nagaraju, B.; Kovvuri, J.; Babu, K.S.; Adiyala, P.R.; Nayak, V.L.; Alarifi, A.; Kamal, A. A facile one pot CC and CN bond formation for the synthesis of spiro-benzodiazepines and their cytotoxicity. *Tetrahedron* **2017**, *73*, 6969–6976. [[CrossRef](#)]
35. Islam, M.S.; Ghawas, H.M.; El-Senduny, F.F.; Al-Majid, A.M.; Elshaier, Y.A.; Badria, F.A.; Barakat, A. Synthesis of new thiazolo-pyrrolidine-(spirooxindole) tethered to 3-acylindole as anticancer agents. *Bioorg. Chem.* **2019**, *82*, 423–430. [[CrossRef](#)]
36. Wu, L.; Liu, Y.; Li, Y. Synthesis of Spirooxindole-O-Naphthoquinone-Tetrazolo [1, 5-a] Pyrimidine Hybrids as Potential Anticancer Agents. *Molecules* **2018**, *23*, 2330. [[CrossRef](#)] [[PubMed](#)]
37. Liu, X.-L.; Feng, T.-T.; Jiang, W.-D.; Yang, C.; Tian, M.-Y.; Jiang, Y.; Lin, B.; Zhao, Z.; Zhou, Y. Molecular hybridization-guided 1, 3-dipolar cycloaddition reaction enabled pyrimidine-fused spiropyrrolidine oxindoles synthesis as potential anticancer agents. *Tetrahedron Lett.* **2016**, *57*, 4411–4416. [[CrossRef](#)]
38. Sudhapriya, N.; Perumal, P.; Balachandran, C.; Ignacimuthu, S.; Sangeetha, M.; Doble, M. Synthesis of new class of spirocarbocycle derivatives by multicomponent domino reaction and their evaluation for antimicrobial, anticancer activity and molecular docking studies. *Eur. J. Med. Chem.* **2014**, *83*, 190–207. [[CrossRef](#)]
39. Liao, S.-R.; Du, L.-J.; Qin, X.-C.; Xu, L.; Wang, J.-F.; Zhou, X.-F.; Tu, Z.-C.; Li, J.; Liu, Y.-H. Site selective synthesis of cytotoxic 1, 3, 6-trisubstituted 3, 6-diunsaturated (3Z, 6Z)-2, 5-diketopiperazines via a one-pot multicomponent method. *Tetrahedron* **2016**, *72*, 1051–1057. [[CrossRef](#)]
40. Abadi, A.H.; Hegazy, G.H.; El-Zaher, A.A. Synthesis of novel 4-substituted-7-trifluoromethylquinoline derivatives with nitric oxide releasing properties and their evaluation as analgesic and anti-inflammatory agents. *Bioorg. Med. Chem.* **2005**, *13*, 5759–5765. [[CrossRef](#)]
41. Liu, J.; Ming, B.; Gong, G.-H.; Wang, D.; Bao, G.-L.; Yu, L.-J. Current research on anti-breast cancer synthetic compounds. *RSC Adv.* **2018**, *8*, 4386–4416. [[CrossRef](#)]
42. Husain, A.; Maaz, M.; Ahmad Ansari, K.; Ahmad, A.; Rashid, M. Synthesis and microbiological evaluation of mannich bases derived from 4, 6-diacetylresorcinol. *J. Chil. Chem. Soc.* **2010**, *55*, 332–334. [[CrossRef](#)]
43. Keri, R.S.; Patil, S.A. Quinoline: A promising antitubercular target. *Biomed. Pharmacother.* **2014**, *68*, 1161–1175. [[CrossRef](#)] [[PubMed](#)]
44. Eswaran, S.; Adhikari, A.V.; Shetty, N.S. Synthesis and antimicrobial activities of novel quinoline derivatives carrying 1, 2, 4-triazole moiety. *Eur. J. Med. Chem.* **2009**, *44*, 4637–4647. [[CrossRef](#)] [[PubMed](#)]
45. Castillo, J.-C.; Jiménez, E.; Portilla, J.; Insuasty, B.; Quiroga, J.; Moreno-Fuquen, R.; Kennedy, A.R.; Abonia, R. Application of a catalyst-free Domino Mannich/Friedel-Crafts alkylation reaction for the synthesis of novel tetrahydroquinolines of potential antitumor activity. *Tetrahedron* **2018**, *74*, 932–947. [[CrossRef](#)]
46. Nandagokula, C.; Poojary, B.; Vittal, S.; Shenoy, S.; Shetty, P.; Tangavelu, A. Synthesis, characterization, and biological evaluation of some N-aryl hydrazones and their 2, 3-disubstituted-4-thiazolidinone derivatives. *Med. Chem. Res.* **2013**, *22*, 253–266. [[CrossRef](#)]
47. Asolkar, R.N.; Schroeder, D.; Heckmann, R.; Lang, S.; Wagner-Doebler, I.; Laatsch, H. Helquinoline, a new tetrahydroquinoline antibiotic from *Janibacter limosus* Hel 1. *J. Antibiot.* **2004**, *57*, 17–23. [[CrossRef](#)]
48. Gudmundsson, K.S.; Boggs, S.D.; Catalano, J.G.; Svolto, A.; Spaltenstein, A.; Thomson, M.; Wheelan, P.; Jenkinson, S. Imidazopyridine-5, 6, 7, 8-tetrahydro-8-quinolinamine derivatives with potent activity against HIV-1. *Bioorg. Med. Chem. Lett.* **2009**, *19*, 6399–6403. [[CrossRef](#)] [[PubMed](#)]

49. Fotie, J.; Kaiser, M.; Delfin, D.A.; Manley, J.; Reid, C.S.; Paris, J.-M.; Wenzler, T.; Maes, L.; Mahasenan, K.V.; Li, C. Antitrypanosomal activity of 1, 2-dihydroquinolin-6-ols and their ester derivatives. *J. Med. Chem.* **2010**, *53*, 966–982. [[CrossRef](#)]
50. Lukevics, E.; Segal, I.; Zablotzkaya, A.; Germane, S. Synthesis and neurotropic activity of novel quinoline derivatives. *Molecules* **1997**, *2*, 180–185. [[CrossRef](#)]
51. Faber, K.; StÜckler, H.; Kappe, T. Non-steroidal antiinflammatory agents. 1. Synthesis of 4-hydroxy-2-oxo-1, 2-dihydroquinolin-3-yl alkanolic acids by the wittig reaction of quinisatines. *J. Heterocycl. Chem.* **1984**, *21*, 1177–1181. [[CrossRef](#)]
52. Jarvest, R.L.; Armstrong, S.A.; Berge, J.M.; Brown, P.; Elder, J.S.; Brown, M.J.; Copley, R.C.; Forrest, A.K.; Hamprecht, D.W.; O'Hanlon, P.J. Definition of the heterocyclic pharmacophore of bacterial methionyl tRNA synthetase inhibitors: Potent antibacterially active non-quinolone analogues. *Bioorg. Med. Chem. Lett.* **2004**, *14*, 3937–3941. [[CrossRef](#)]
53. Bendale, P.; Olepu, S.; Suryadevara, P.K.; Bulbule, V.; Rivas, K.; Nallan, L.; Smart, B.; Yokoyama, K.; Ankala, S.; Pendyala, P.R. Second generation tetrahydroquinoline-based protein farnesyltransferase inhibitors as antimalarials. *J. Med. Chem.* **2007**, *50*, 4585–4605. [[CrossRef](#)]
54. Gholap, A.R.; Toti, K.S.; Shirazi, F.; Kumari, R.; Bhat, M.K.; Deshpande, M.V.; Srinivasan, K.V. Synthesis and evaluation of antifungal properties of a series of the novel 2-amino-5-oxo-4-phenyl-5, 6, 7, 8-tetrahydroquinoline-3-carbonitrile and its analogues. *Bioorg. Med. Chem.* **2007**, *15*, 6705–6715. [[CrossRef](#)]
55. Liou, J.-P.; Wu, Z.-Y.; Kuo, C.-C.; Chang, C.-Y.; Lu, P.-Y.; Chen, C.-M.; Hsieh, H.-P.; Chang, J.-Y. Discovery of 4-amino and 4-hydroxy-1-aryloxyindoles as potent tubulin polymerization inhibitors. *J. Med. Chem.* **2008**, *51*, 4351–4355. [[CrossRef](#)] [[PubMed](#)]
56. Tramontini, M. Advances in the chemistry of Mannich bases. *Synthesis* **1973**, *1973*, 703–775. [[CrossRef](#)]
57. Malinakova, H.C. Multicomponent Reaction Sequences Using Palladacyclic Complexes. In *Palladacycles*; Elsevier: Amsterdam, The Netherlands, 2019; pp. 263–295.
58. Paprocki, D.; Madej, A.; Koszelewski, D.; Brodzka, A.; Ostaszewski, R. Multicomponent reactions accelerated by aqueous micelles. *Front. Chem.* **2018**, *6*, 502. [[CrossRef](#)] [[PubMed](#)]
59. Malinakova, H.C. Recent advances in the discovery and design of multicomponent reactions for the generation of small-molecule libraries. *Rep. Org. Chem.* **2015**, *5*, 75–90. [[CrossRef](#)]
60. Weber, L. The application of multi-component reactions in drug discovery. *Curr. Med. Chem.* **2002**, *9*, 2085–2093. [[CrossRef](#)] [[PubMed](#)]
61. Mannich, C.; Krösche, W. Ueber ein kondensationsprodukt aus formaldehyd, ammoniak und antipyrin. *Arch. Pharm.* **1912**, *250*, 647–667. [[CrossRef](#)]
62. Blicke, F. The Mannich Reaction. *Org. React.* **2004**, *1*, 303–341.
63. Lipinski, C.A.; Lombardo, F.; Dominy, B.W.; Feeney, P.J. Experimental and computational approaches to estimate solubility and permeability in drug discovery and development settings. *Adv. Drug Deliv. Rev.* **1997**, *23*, 3–25. [[CrossRef](#)]
64. Benet, L.Z.; Hosey, C.M.; Ursu, O.; Oprea, T.I. BDDCS, the rule of 5 and drugability. *Adv. Drug Deliv. Rev.* **2016**, *101*, 89–98. [[CrossRef](#)] [[PubMed](#)]
65. Lipinski, C.A. Drug-like properties and the causes of poor solubility and poor permeability. *J. Pharmacol. Toxicol. Methods* **2000**, *44*, 235–249. [[CrossRef](#)]
66. Rahman, L.; Shinwari, Z.K.; Iqar, I.; Rahman, L.; Tanveer, F. An assessment on the role of endophytic microbes in the therapeutic potential of *Fagonia indica*. *Ann. Clin. Microbiol. Antimicrob.* **2017**, *16*, 53. [[CrossRef](#)]
67. Seelolla, G.; Cheera, P.; Ponneri, V. Synthesis, antimicrobial and antioxidant activities of novel series of cinnamamide derivatives having morpholine moiety. *Med. Chem.* **2014**, *4*, 778–783. [[CrossRef](#)]
68. Katbab, A.; Scott, G. Mechanisms of antioxidant action: The involvement of nitroxyl radicals in the antifatigue action of secondary amines. *Eur. Polym. J.* **1981**, *17*, 559–565. [[CrossRef](#)]
69. Mistry, B.; Patel, R.V.; Keum, Y.-S.; Kim, D.H. Synthesis of N-Mannich bases of berberine linking piperazine moieties revealing anticancer and antioxidant effects. *Saudi J. Biol. Sci.* **2017**, *24*, 36–44. [[CrossRef](#)]
70. Prieto, P.; Pineda, M.; Aguilar, M. Spectrophotometric Quantitation of Antioxidant Capacity through the Formation of a Phosphomolybdenum Complex: Specific Application to the Determination of Vitamin E. *Anal. Biochem.* **1999**, *269*, 337–341. [[CrossRef](#)]

71. Kanzler, C.; Haase, P.T.; Schestkova, H.; Kroh, L.W. Antioxidant properties of heterocyclic intermediates of the Maillard reaction and structurally related compounds. *J. Agric. Food Chem.* **2016**, *64*, 7829–7837. [[CrossRef](#)]
72. Singh, N.; Rajini, P. Free radical scavenging activity of an aqueous extract of potato peel. *Food Chem.* **2004**, *85*, 611–616. [[CrossRef](#)]
73. Semon, W.L. Antioxidant. U.S. Patent No. 2,166,223, 18 July 1939.
74. Shahidi, F.; Janitha, P.; Wanasundara, P. Phenolic antioxidants. *Crit. Rev. Food Sci. Nutr.* **1992**, *32*, 67–103. [[CrossRef](#)]
75. El-Gohary, N.; Shaaban, M. Antimicrobial and antiquorum-sensing studies. Part 2: Synthesis, antimicrobial, antiquorum-sensing and cytotoxic activities of new series of fused [1, 3, 4] thiaziazole and [1, 3] benzothiazole derivatives. *Med. Chem. Res.* **2014**, *23*, 287–299. [[CrossRef](#)]
76. Solis, P.N.; Wright, C.W.; Anderson, M.M.; Gupta, M.P.; Phillipson, J.D. A microwell cytotoxicity assay using *Artemia salina* (brine shrimp). *Planta Med.* **1993**, *59*, 250–252. [[CrossRef](#)]
77. Birndorf, H.C.; D'Alessio, J.; Bagshaw, J.C. DNA-dependent RNA-polymerases from *Artemia* embryos: Characterization of polymerases I and II from nauplius larvae. *Dev. Biol.* **1975**, *45*, 34–43. [[CrossRef](#)]
78. Sanchez, C.; Gupta, M.; Vasquez, M.; Montenegro, G. Bioassay with brine *Artemia* to predict antibacterial and pharmacologic activity. *Rev. Med. Panama* **1993**, *18*, 62–69.
79. Das, S.; da Silva, C.J.; Silva, M.d.M.; Dantas, M.D.d.A.; de Fátima, Â.; Ruiz, A.L.T.G.; da Silva, C.M.; de Carvalho, J.E.; Santos, J.C.; Figueiredo, I.M. Highly functionalized piperidines: Free radical scavenging, anticancer activity, DNA interaction and correlation with biological activity. *J. Adv. Res.* **2018**, *9*, 51–61. [[CrossRef](#)]
80. Abdo, N.Y.M.; Kamel, M.M. Synthesis and anticancer evaluation of 1, 3, 4-oxadiazoles, 1, 3, 4-thiadiazoles, 1, 2, 4-triazoles and Mannich bases. *Chem. Pharm. Bull.* **2015**, *63*, 369–376. [[CrossRef](#)]
81. Wiji Prasetyaningrum, P.; Bahtiar, A.; Hayun, H. Synthesis and cytotoxicity evaluation of novel asymmetrical mono-carbonyl analogs of curcumin (AMACs) against Vero, HeLa, and MCF7 Cell Lines. *Sci. Pharm.* **2018**, *86*, 25. [[CrossRef](#)]
82. Kumar, G.S.; Prasad, Y.R.; Mallikarjuna, B.; Chandrashekar, S. Synthesis and pharmacological evaluation of clubbed isopropylthiazole derived triazolothiadiazoles, triazolothiadiazines and mannich bases as potential antimicrobial and antitubercular agents. *Eur. J. Med. Chem.* **2010**, *45*, 5120–5129. [[CrossRef](#)] [[PubMed](#)]
83. Dimmock, J.R.; Vashishtha, S.C.; Quail, J.W.; Pugazhenth, U.; Zimpel, Z.; Sudom, A.M.; Allen, T.M.; Kao, G.Y.; Balzarini, J.; De Clercq, E. 4-(β -Arylvinyloxy)-3-(β -arylvinyloxy)-1-ethyl-4-piperidinols and Related Compounds: A Novel Class of Cytotoxic and Anticancer Agents. *J. Med. Chem.* **1998**, *41*, 4012–4020. [[CrossRef](#)]
84. Rao, U.M.; Ahmad, B.A.; Mohd, K.S. In vitro nitric oxide scavenging and anti-inflammatory activities of different solvent extracts of various parts of *Musa paradisiaca*. *Malays. J. Anal. Sci.* **2016**, *20*, 1191–1202. [[CrossRef](#)]
85. Koksall, M.; Ozkan-Dagliyan, I.; Ozyazici, T.; Kadioglu, B.; Sipahi, H.; Bozkurt, A.; Bilge, S.S. Some Novel Mannich Bases of 5-(3, 4-Dichlorophenyl)-1, 3, 4-oxadiazole-2 (3H)-one and Their Anti-Inflammatory Activity. *Arch. Pharm.* **2017**, *350*, 1700153. [[CrossRef](#)] [[PubMed](#)]
86. Ames, B.N.; Shigenaga, M.K.; Hagen, T.M. Oxidants, antioxidants, and the degenerative diseases of aging. *Proc. Natl. Acad. Sci. USA* **1993**, *90*, 7915–7922. [[CrossRef](#)] [[PubMed](#)]
87. Chu, Y.-F.; Sun, J.; Wu, X.; Liu, R.H. Antioxidant and antiproliferative activities of common vegetables. *J. Agric. Food Chem.* **2002**, *50*, 6910–6916. [[CrossRef](#)] [[PubMed](#)]
88. Simmons, D.L.; Wagner, D.; Westover, K. Nonsteroidal anti-inflammatory drugs, acetaminophen, cyclooxygenase 2, and fever. *Clin. Infect. Dis.* **2000**, *31*, S211–S218. [[CrossRef](#)]
89. SwissADME Software. Available online: <http://swissadme.ch/index.php> (accessed on 8 January 2020).
90. Tai, Z.; Cai, L.; Dai, L.; Dong, L.; Wang, M.; Yang, Y.; Cao, Q.; Ding, Z. Antioxidant activity and chemical constituents of edible flower of *Sophora viciifolia*. *Food Chem.* **2011**, *126*, 1648–1654. [[CrossRef](#)]
91. Aguilar Urbano, M.; Pineda Priego, M.; Prieto, P. Spectrophotometric quantitation of antioxidant capacity through the formation of a phosphomolybdenum complex: Specific application to the determination of vitamin E1. *Anal. Biochem.* **2013**, *269*, 337–341.

92. Khan, K.; Fatima, H.; Taqi, M.M.; Zia, M.; Mirza, B. Phytochemical and in vitro biological evaluation of *Artemisia scoparia* Waldst. & Kit for enhanced extraction of commercially significant bioactive compounds. *J. Appl. Res. Med. Aromat. Plants* **2015**, *2*, 77–86. [[CrossRef](#)]
93. Kim, J.-S.; Kwon, C.-S.; SoN, K.H. Inhibition of alpha-glucosidase and amylase by luteolin, a flavonoid. *Biosci. Biotechnol. Biochem.* **2000**, *64*, 2458–2461. [[CrossRef](#)] [[PubMed](#)]
94. Meyer, B.; Ferrigni, N.; Putnam, J.; Jacobsen, L.; Nichols, D.J.; McLaughlin, J.L. Brine shrimp: A convenient general bioassay for active plant constituents. *Planta Med.* **1982**, *45*, 31–34. [[CrossRef](#)] [[PubMed](#)]
95. Khan, S.; Shin, E.M.; Choi, R.J.; Jung, Y.H.; Kim, J.; Tosun, A.; Kim, Y.S. Suppression of LPS-induced inflammatory and NF- κ B responses by anomalin in RAW 264.7 macrophages. *J. Cell. Biochem.* **2011**, *112*, 2179–2188. [[CrossRef](#)]
96. Zhang, H.; Wang, X.; Mao, J.; Huang, Y.; Xu, W.; Duan, Y.; Zhang, J. Synthesis and biological evaluation of novel benzofuroxan-based pyrrolidine hydroxamates as matrix metalloproteinase inhibitors with nitric oxide releasing activity. *Bioorg. Med. Chem.* **2018**, *26*, 4363–4374. [[CrossRef](#)] [[PubMed](#)]
97. Ahn, K.S.; Noh, E.J.; Zhao, H.L.; Jung, S.H.; Kang, S.S.; Kim, Y.S. Inhibition of inducible nitric oxide synthase and cyclooxygenase II by Platycodon grandiflorum saponins via suppression of nuclear factor- κ B activation in RAW 264.7 cells. *Life Sci.* **2005**, *76*, 2315–2328. [[CrossRef](#)] [[PubMed](#)]
98. Zeeshan, S.; Naveed, M.; Khan, A.; Atiq, A.; Arif, M.; Ahmed, M.N.; Kim, Y.S.; Khan, S. N-Pyrazoloyl and N-thiopheneacetyl hydrazone of isatin exhibited potent anti-inflammatory and anti-nociceptive properties through suppression of NF- κ B, MAPK and oxidative stress signaling in animal models of inflammation. *Inflamm. Res.* **2019**, *68*, 613–632. [[CrossRef](#)] [[PubMed](#)]

Sample Availability: Samples of the compounds are available from the authors.



© 2020 by the authors. Licensee MDPI, Basel, Switzerland. This article is an open access article distributed under the terms and conditions of the Creative Commons Attribution (CC BY) license (<http://creativecommons.org/licenses/by/4.0/>).